horticulturae

MDPI

Article

Volatile Profiles of Vidal Grapes in the Shangri-La High-Altitude Region during On-Vine Non-Destructive Dehydration

Qing-Fang Xu [1,†], Liang Fan [1,2,†], Kai-Xiang Lu [1,3], Dong-Mei Zhao [1,3], Ming-Xia Zhang [2] and Jian Cai [1,*]

[1] Yunnan Engineering Research Center of Fruit Wine, Qujing Normal University, Qujing 655011, China
[2] School of Life Science and Technology, Henan Institute of Science and Technology, Xinxiang 453003, China
[3] College of Food Science and Technology, Yunnan Agricultural University, Kunming 650500, China
* Correspondence: caijian928@outlook.com; Tel.: +86-874-8998627
† These authors contributed equally to this work.

Abstract: Both free and glycosidically bound forms of volatile compounds in Vidal grapes from the Shangri-La high-altitude region during the on-vine non-destructive dehydration process were investigated by headspace solid-phase micro-extraction (HS-SPME) combined with gas chromatography–mass spectrometry (GC-MS), following which the data were processed by multivariate statistical analysis. Fatty-acid-derived volatiles (FADs), amino-acid-derived volatiles (AADs), and isoprene-derived volatiles (IPDs), which occurred mainly in bound forms, were the three major volatiles in dehydrated Vidal grapes. Water-loss concentration, biosynthesis, and biodegradation all occurred during dehydration, eventually modifying some volatiles significantly, especially some powerful odorants such as hexanal, *trans*-2-hexenal, 2-phenethyl acetate, β-myrcene, linalool, geraniol, *cis*-rose oxide, and β-damascenone. 1-Octen-3-ol was relatively stable during the non-destructive on-vine dehydration process and its content in grape juice was mainly determined by the concentration effect. 2,4-Di-*tert*-butylphenol, 2-phenethyl acetate, 2-methyl-1-propanol, and hexanol were screened as some of the most important metabolic markers to discriminate grapes at different dehydration degrees. Our study also highlights the fundamental importance of the expression of volatile content in the metabolomic study of grape berries.

Keywords: late harvest; over-ripening; dessert wine; metabolomics; clustered heatmap; OPLS-DA

Citation: Xu, Q.-F.; Fan, L.; Lu, K.-X.; Zhao, D.-M.; Zhang, M.-X.; Cai, J. Volatile Profiles of Vidal Grapes in the Shangri-La High-Altitude Region during On-Vine Non-Destructive Dehydration. *Horticulturae* **2022**, *8*, 1029. https://doi.org/10.3390/horticulturae8111029

Academic Editor: Carlos M. Lopes

Received: 7 October 2022
Accepted: 2 November 2022
Published: 3 November 2022

1. Introduction

Volatile compounds are mainly present as free and bound forms in grape skins and pulp, and they are the main source of aromatic components in grape juice and wine [1]. These compounds are transferred to the wine during the winemaking process and, together with the volatiles produced by the microorganisms during fermentation, form the wine aroma [2]. Therefore, the volatile composition of the original grape berries plays an important role in the formation of the organoleptic quality of the final wine [3]. As secondary metabolites of grape berries, volatile compounds are mainly derived from fatty acids, amino acids, and isoprenes [2,4]. These secondary metabolites are mainly influenced by the grape variety, ecological conditions, viticultural management practices, maturity degree, and even late or postharvest technologies [2,4].

The Shangri-La region, located in southwest China, is an excellent and unique wine region, characterized by its diverse sub-climatic conditions formed under low-latitude and high-altitude (average elevation above 2000 m) geographical environments [5,6]. This region produces a wide variety of wines, including the most common red and white dry wines, late-harvest dessert wines, botrytized wines, and even icewines from some vineyards at particularly high elevations. The wine grape varieties grown in this region mainly include Cabernet Sauvignon, Merlot, Syrah, Rose Honey, Crystal Grape, Vidal, and so on [5,7,8]. Benefiting from the dry climate after technological maturing, late-harvest

wines are widely made in the dry-hot wine region valleys in Shangri-La. For example, in Weixi county (Diqing, Yunnan Province), Vidal grapes are always harvested at the end of December or early January, when the total soluble solids exceed 30° Brix by on-vine natural dehydration, with which late-harvest dessert wines are made. However, the volatile compound profile of Vidal grapes in this region has not been extensively investigated to date, especially regarding the late-harvest on-vine dehydration process.

It is well-known that wines made from late-harvested or post-harvest dehydrated grapes have higher sugar levels and more intense flavors than wines made from grapes of normal maturity [9,10]. Many researchers and winemakers attribute these results to the dehydration and concentration effect of the grape berries during these processes [11]. Indeed, the pre-fermentation 'concentration' process (either natural or artificial) not only concentrates the grape juice, but also changes the grape's secondary metabolism and the content of flavors, ultimately affecting the sensory quality of the final wine [12]. The pre-fermentation dehydration process includes both on-vine (over-ripening, icing, and *Botrytis*) and off-vine (natural and artificial drying) processes [10]. The evolution of volatile compounds is determined by many factors, such as the dehydration model (on-vine or off-vine) [13], grape variety [14], water-loss technology [15], drying temperature [16], environmental factors [10], and even the microeukaryotic community [17]. Oxidation and anaerobic metabolism have also been observed in grape berries during the off-vine dehydration and on-vine icing processes [18–20].

It should be pointed out that the berry dehydration that happened during the late-harvest process of noble-rotted and icewine grapes is actually a structurally destructive dehydration process for grape berries. For noble-rotted grapes after *Botrytis* infection, the pectin of the cell wall is degraded, and the affected tissue is collapsed due to the presence of destructive pectolytic enzymes. This structural disruption promotes berry dehydration under dry weather conditions [12]. For icewine making, the grapes undergo a dehydration process and endure several freeze–thaw cycles during the late-harvest freezing process, accelerating disruption of the berry cellular structure and leading to damage to the grape skin wax layer [17,19,21].

As reviewed above, most of the studies in the existing literature have focused on the grape aroma evolution during destructive dehydration and off-vine post-harvest drying processes, while little research has been conducted on the non-destructive dehydration process during on-vine late-harvest. Furthermore, the ecological condition is the main influencing factor on the variation trend of aromatic compounds during grape dehydration [10], and the accumulation of volatile compounds in Vidal grapes of the Weixi high-altitude wine region has not been investigated before. Therefore, the target of this study was to explore the influence of the on-vine non-destructive dehydration degree on both free and glycosidically bound volatile compounds in Vidal grapes. We expect that the results of this study will help winemakers to make better-informed decisions on the final harvest date, regarding the balance between grape juice yield and wine aroma quality.

2. Materials and Methods

2.1. Vineyard and Sampling Information

The Vidal late-harvest grapes in this research came from a commercial vineyard in Weixi County, Diqing Tibetan Autonomous Prefecture, Yunnan province, China. The vineyard is located at the foot of Yongchun River Valley (27°7′ N, 99°22′ E), on a southwest-oriented slope of about 30° with an altitude of 2400 to 2450 m. The grapevines were planted own-rooted in 2012 with a planting density of 2.5 × 2 m, using a VSP trellising system with east–west rows perpendicular to the slope. The vines were pruned with five to six shoots and the yield was controlled at about 9000 kg/ha at technical maturity.

More than 1500 grape berries were collected by hand randomly from at least 100 different grapevines at every sampling point. The meteorological data during late-harvest was downloaded from the China National Meteorological Science Data Sharing Center (http://data.cma.cn (accessed on 1 June 2022)). None of the grapes were infected by *Botrytis*

cinerea or had suffered from freeze–thaw cycles before harvest, which means that they had undergone a non-destructive on-vine late-harvest process. Based on the phenological period and dehydration progress of Vidal grapes in previous vintages, five sampling points were set at 14-day intervals, starting after technical maturation and from the beginning of the dehydration process. The sampling dates were 28 October, 12 and 27 November, and 12 and 27 December (abbreviated as T1, T2, T3, T4, and T5, respectively). Grape berries were transported to the winery laboratory for physicochemical index analysis and the rest of them were frozen with liquid nitrogen and stored at −40 °C for subsequent volatile compounds analysis within 3 months after sampling. The visual appearance of the grapes after harvest at T5 is shown in Figure S2.

2.2. Physicochemical Parameters Analysis

Three replicates of 100 randomly selected berries from each sampling point were pressed and the grape juice was centrifuged using a refrigerated centrifuge (TGL-16M, CENCE, Changsha, China) in 50 mL centrifugal tubes at 6000 rpm for 10 min at 4 °C, for physicochemical index analysis. The berry weight and juice weight were directly measured using an electronic balance with an accuracy of 0.1 mg (FA1004B, Shanghai Yueping, Shanghai, China). Juice volume per 100 berries was directly measured using a 100 mL glass cylinder with accuracy of 0.1 mL (BOMEX, Beijing, China) after centrifugation during volatile extraction (detailed in Section 2.3.1). Juice yield (%) was calculated by dividing the juice weight by the berry weight. Berry weight loss (%) was equal to the difference in berry weight between the sampling point and T1, divided by the berry weight of T1. Total soluble solids (TSS) was measured using a digital refractometer (Pocket Refractometer Pal-1, Atago, Tokyo, Japan). Other common quality parameters, such as total sugar concentration, pH value, and titratable acidity, were analyzed using the methods described in the National Standard of the People's Republic of China (GB/T15038-2006) [22].

2.3. Free and Bound Volatile Compounds Analysis

According to the method described by Lan et al. (2016) [19], the free and glycosidically bound volatile compounds from grape berries were extracted and analyzed by gas chromatography–mass spectrometry (GC-MS) for identification and quantification. The used method is summarized in the following.

2.3.1. Extraction of Free and Bound Volatile Compounds

Under the protection of liquid nitrogen, all seeds were removed from 100 grape berries. One gram of PVPP (polyvinylpolypyrrolidone) (Aladdin Biochemical Technology, Shanghai, China) and 0.5 g of D-gluconic acid lactone (Yuanye Bio-Technology, Shanghai, China) were added to the frozen flesh. After being ground to a powder in a ceramic mortar and macerated for 4 h at 4 °C in 50 mL centrifugal tubes, the mixture was centrifuged at 6000 rpm for 10 min at the same temperature. Then, the clarified juice was collected into 20 mL screw-caped glass sample bottles (ANPEL Laboratory Technologies, Shanghai, China). The weight of 100 berries and the volume of all pressed juice were measured simultaneously, as described in Section 2.2.

Free volatile compounds were directly extracted by an automatic sampler for headspace solid-phase microextraction (HS-SPME).

The extraction of glycosidically bound volatile compounds from the clarified juice obtained above included three steps: glycosides collection, enzymatic hydrolysis, and HS-SPME. The glycosides were isolated from grape juice using Cleanert PEP-SPE resins (200 mg/6 mL; Agela, CA, USA) previously conditioned with chromatographic-grade methanol (Aladdin Biochemical Technology, Shanghai, China) and Milli-Q water (prepared by a laboratory ultrapure water machine, Lake Intelligent Precision Instrument, Shenzhen, China). Two milliliters of clarified juice were passed through the SPE column, and 5 mL Milli-Q water was added to remove sugars, acids, and other polar compounds. Then, 5 mL dichloromethane of chromatographic grade (Merck KGaA, Darmstadt, Germany) was

added, in order to eliminate the free-form volatiles. Finally, the glycoside fractions were eluted with 20 mL methanol. Five eluants were gathered together to evaporate to dryness under a nitrogen stream, then re-dissolved in 10 mL citrate–phosphate buffer (0.2 M, pH 5.0, Yuanye Bio-Technology, Shanghai, China). After 100 µL of AR2000 glycosidase (Rapidase, 100 g/L, Creative Enzymes, NY, USA) was added, enzymolysis was activated in 20 Ml glass vials for 16 h at 40 °C in a constant temperature water bath (SHZ-88, Changzhou Jintanwenhua, Changzhou, China). The released odorants were extracted by HS-SPME, as before.

2.3.2. HS-SPME Conditions

One gram of sodium chloride (Yuanye Bio-Technology, Shanghai, China) and 20 µL internal standard of 1,3-dimethyl-1-butanol (2000 µg/L, Sigma–Aldrich, MO, USA) were added to 5 mL of juice sample in a 20 mL sampling vial, which was sealed by a cap with PTFE-silicon septum (ANPEL Laboratory Technologies, Shanghai, China) immediately and equilibrated at 40 °C for 0.5 h in the heating module of the automatic HS-SPME sampler (PAL RSI 85, CTC Analytics, Zwingen, Switzerland). The solid-phase microextraction was conducted using a 2 cm fiber (PDMS/CAR/DVB, Supelco, Bellefonte, PA, USA), which was previously heat-activated (at 250 °C), and then was inserted into the vial for extraction for 0.5 h at 40 °C with stirring in the heating/stirring module. Finally, the fiber was injected into the GC inlet for 8 min of thermal desorption (250 °C).

2.3.3. GC-MS Analysis

The separation and identification of grape volatiles were carried out using an Agilent 7890B GC and 5977B MS with the same HP-INNOWAX capillary column (J&W Scientific, Folsom, CA, USA) as in the referenced method. The inlet temperature was controlled at 250 °C and the injection mode was splitless. High-purity helium (>99.999%, WinTec Specialty Gas, Sichuan, China) was used as the carrier gas, with a 1 mL/min flow rate. The oven temperature started from 50 °C for 1 min, increased to 220 °C at 3 °C/min, and held for 5 min. The temperatures of the transfer line heater, ion source, and quadrupole were 250 °C, 250 °C, and 150 °C, respectively. Electron ionization (EI) was applied at 70 eV for the mass detector in full-scan mode (m/z 30–350).

2.3.4. Identification and Quantification of Volatile Compounds

The data from GC-MS analysis were processed using Agilent MSD ChemStation software. Compounds were identified according to their reference standards, retention indices (RI), and the mass spectra in the standard NIST 17 library. According to the quality parameters of the grape samples, a synthetic model juice solution (glucose 250 g/L, tartaric acid 7 g/L, and pH 3.0) was prepared for the quantitative calibration curves. The solution of dissolved and mixed standards was diluted into 15 levels in succession using the model juice. Each level of the standard solution was treated and analyzed with the same HS-SPME GC-MS method described above. Compounds without available standards were tentatively quantified according to their analogs. The contents of free and glycosidically bound volatile compounds are expressed as both µg/L and ng/berry. The latter expression of content was calculated by multiplying the former by the volume of sample juice, then dividing by the number of sample berries. The total content of each volatile compound was calculated as the sum of its free and bound forms.

2.4. Data Processing and Statistical Analysis

The preliminary processing of data and plotting of the physicochemical parameters were performed using Microsoft Excel 2016 software. The one-way analysis of variance (ANOVA) and unary linear regression analysis (U-LRA) were performed with IBM SPSS Statistics 19 software. The ANOVA was based on the Duncan test at a significance level of $p < 0.05$. Hierarchical clustering heatmaps were obtained from MetaboAnalyst 5.0 (http://www.metaboanalyst.ca (accessed on 1 June 2022)) using the 'Statistical Analysis'

module. The 'Autoscaling' method was used as the normalization procedure for data before proceeding. Principal component analysis (PCA) and orthogonal partial least-squares discriminant analysis (OPLS-DA) were performed using SIMCA 14.1 (Umetrics, Umeå Sweden).

3. Results and Discussion

3.1. Physicochemical Parameters

The evolution of the basic quality parameters during the on-vine late-harvest dehydration of Vidal grapes is depicted in Figure 1. It should be noticed that the sugar and titrated acid content are represented in two ways, namely, as 'g/L' for juice and as 'g/berry' for the total amount per single berry.

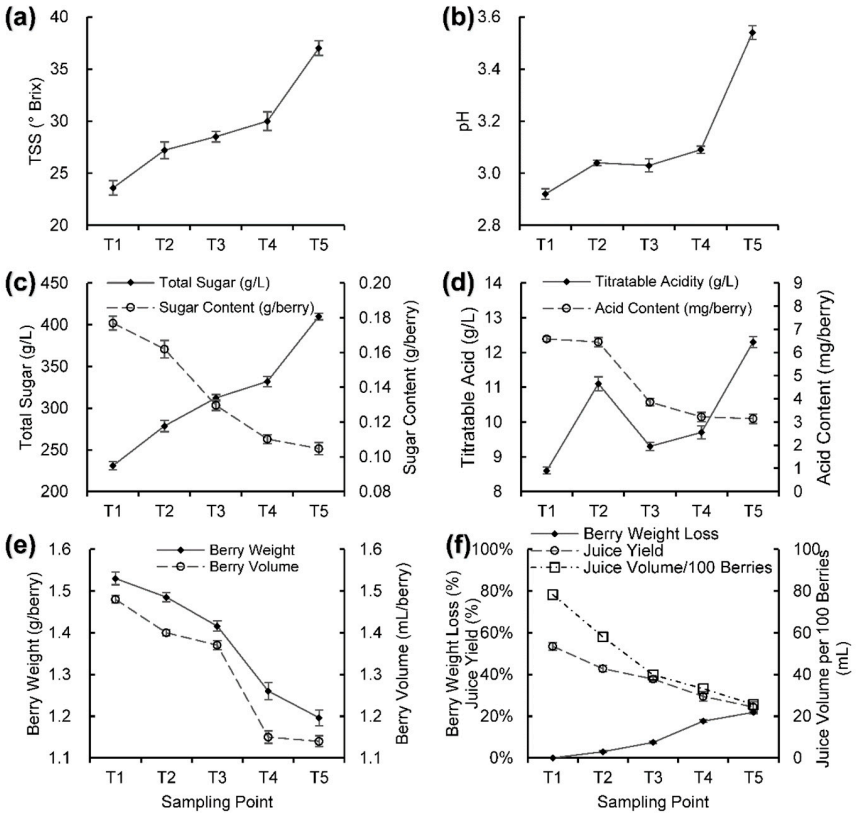

Figure 1. Physicochemical parameters during the on-vine dehydration process of Vidal grapes. T1, T2, T3, T4, and T5 represent the sampling points at different dehydration degrees. Values are the means of three replicates. The error bars represent the standard deviation. (**a**) Total Soluble Solid (TSS); (**b**) pH; (**c**) Total Sugar and Sugar Content; (**d**) Titratable Acid and Acid Content; (**e**) Berry Weight and Berry Volume; (**f**) Berry Weight Loss, Juice Yield, and Juice Volume per 100 Berries.

The substantial reductions in berry weight (BW) and berry volume (BV) throughout the sampling period suggested that typical natural dehydration occurred during this process (Figure 1e). At T5, the BW was only 78.2% that at T1, and the BV was only 77.0% that at T1. A berry weight loss (BWL) of 21.8% was caused by on-vine dehydration, which directly reflected the level of berry water loss. In our opinion, it is not appropriate to express BWL (%) as berry water loss (%), as in some articles [19,23], because water loss (%) is the percentage of lost water in the net water content in grape berries, while BWL (%) is the percentage of lost water in the whole weight of the grape berry. The increasing trend in BWL (Figure 1f) indicated that the water loss proceeded more effectively in the later stages of the sampling period, due to the drier weather and more wind in this period (see the meteorological data shown in Figure S1). Adequate sunshine and a windy, cool, dry climate not only ensured the slow and continuous on-vine dehydration of the grapes, but

also protected them from fungal infections. Some authors have proposed that the rate of water loss and dehydration temperature have an important influence on the phenolic and volatile compounds in the grape berries and even in the final wines [10,14,24].

Juice yield (%) (calculated in mass percent) and juice volume per 100 berries (JV100) are shown in Figure 1f. After two months of natural on-vine dehydration, the juice yield (%) of Vidal grapes reduced by 54.4%, from 53.5% to 24.4%. The JV100 reduced from 76.6 mL to 25.6 mL after this process, indicating a 66.6% reduction in final wine production.

There is no doubt that lower yields lead to higher quality. The total sugar concentration (g/L) and TSS (°Brix) of the juice were enhanced dramatically by the on-vine water-loss process (Figure 1a,c). The sharp increase in sugar concentration in grape juice between T4 and T5 provides further evidence that the water-loss rate was much higher in the later stage of dehydration. However, even though the pH value increased continuously, the titratable acid concentration in the grape juice showed different patterns during the dehydration process, presenting fluctuating changes (Figure 1b,d). The low pH of Vidal grapes at technical maturation in the Weixi region has led to a series of winemaking problems, an essential reason why this variety is used to make late-harvest dessert wines in this region. On-vine dehydration provides a good solution to the low pH problem in this area, as can be seen from our results. The enhancement of the sugar content and the fluctuation in acidity were consistent with the results of previous studies on icewine grapes [19] and postharvest off-vine drying grapes [11]. Bowen et al. (2015) [25] have attributed the reduction in must acidity during icewine grape late-harvest to the precipitation of potassium tartrate caused by on-vine freeze–thaw cycles. However, the temperature data in Figure S1a indicate that the Vidal grapes in our study did not suffer from freeze–thaw cycles.

Nevertheless, the situation was different when considering the total content of sugars and acids in a single berry. Their total content in each berry showed a constant decrease during on-vine dehydration, with the sugars decreasing by 40.7% and the titratable acids by 52.3% (Figure 1c,d). This result suggests that both water-loss concentration and biodegradation happened simultaneously during the on-vine natural dehydration of Vidal grapes. As acids were degraded more rapidly, fluctuations in the juice appeared in the early dehydration stages. The concentration of both sugars and acids increased significantly at T5, indicating that the concentration effect was greater than that of degradation throughout the whole process. Chkaiban et al. (2007) [26] have suggested that the increase or decrease in must acidity during grape dehydration is determined by the temperature or water-loss rate, where rapid dehydration mainly enhances acidity. Their studies also indicated that the decrease in acidity at the beginning of dehydration is mainly due to the catabolism of malic acid. Our result was well-explained by this perspective. The continuous decrease in the titratable acid content per berry was due to the natural dehydration occurring at a lower rate. A reduction in sugar content per berry during dehydration has also been observed by Mencarelli et al. (2013) [10], who found that the concentration effect was partially reduced by sugar respiration in some Italian grape varieties during dehydration.

3.2. Volatile Profiles of Vidal Grapes in Weixi Region after On-Vine Dehydration (T5)

The detailed qualitative and quantitative information are listed in Table 1. A total of 100 volatile compounds were identified as free or glycosidically bound forms in the Weixi region Vidal grapes at harvest (T5) after on-vine dehydration in this study, including fatty-acid-derived volatiles (FADs), amino-acid-derived volatiles (AADs), isoprenoid-derived volatiles (IPDs), furan compounds (FCs), and other compounds. In order to better demonstrate the overall aroma potential of the grape berries, the total volatile contents were calculated, equal to the sum of the free and bound volatile compounds. The quantitative result is shown in Table S1. From a viticultural point of view, the contents of volatiles are also expressed as ng/berry, in order to avoid the dilution or concentration effects mentioned by some authors [10,19], and the data are shown in Table S2. As shown in Figure 2, FADs, AADs, and IPDs were the three main groups of volatile compounds in both free and bound forms in Vidal grapes after on-vine dehydration (T5); these compounds existed mainly in bound forms.

Table 1. Qualitative and quantitative information of the volatile compounds.

Compounds	CAS	RI Calculated	RI in Literatures	Quantitative Ion (*m*/*z*)	Identification *	Purity of Standards	Manufacturers of Standards	Quantitative Standards	Calibration Curves	R^2
Ethanol	64-17-5	944	943	31	A	99%	Sigma–Aldrich	A **	Y = 0.1135 × X − 0.0016	0.9982
Acetaldehyde	75-07-0	714	714	29	A	99%	Sigma–Aldrich	A	Y = 1.3283 × X − 0.0314	0.9989
Acetic acid	64-19-7	1477	1476	43	A	99%	Sigma–Aldrich	A	Y = 1.5206 × X − 0.0363	0.9966
Ethyl Acetate	141-78-6	898	896	43	A	99%	Sigma–Aldrich	A	Y = 9.598 × X − 0.0131	0.9996
Hexanol	111-27-3	1359	1356	56	A	98%	Sigma–Aldrich	A	Y = 2.3556 × X + 0.0017	0.9998
trans-3-Hexenol	928-97-2	1371	1372	41	A	97%	Sigma–Aldrich	A	Y = 0.8062 × X − 0.0002	0.9983
cis-3-Hexenol	928-96-1	1393	1393	67	A	98%	Sigma–Aldrich	A	Y = 0.5711 × X − 0.0015	0.9998
trans-2-Hexenol	928-95-0	1411	1412	57	A	97%	Sigma–Aldrich	A	Y = 1.1561 × X + 0.005	0.9991
cis-2-Hexenol	928-94-9	1421	1418	57	B			*trans*-2-Hexenol	Y = 1.1561 × X + 0.005	0.9991
Nonyl alcohol	143-08-8	1668	1664	56	B			Octanol	Y = 0.16169 × X − 0.027	0.9957
cis-6-Nonenol	35854-86-5	1694	1696	55	B			Octanol	Y = 0.16169 × X − 0.027	0.9957
Butanol	71-36-3	1148	1147	56	A	99%	Sigma–Aldrich	A	Y = 0.1135 × X − 0.0016	0.9982
Pentanol	71-41-0	1255	1259	55	A	99%	Sigma–Aldrich	A	Y = 0.457 × X − 0.0001	0.9998
Heptanol	111-70-6	1463	1463	70	A	98%	Sigma–Aldrich	A	Y = 7.3243 × X − 0.008	0.9995
Octanol	111-87-5	1564	1562	56	A	99%	Sigma–Aldrich	A	Y = 0.16169 × X − 0.027	0.9957
Decanol	112-30-1	1769	1766	70	A	99%	Sigma–Aldrich	A	Y = 0.0025 × X + 0.0004	0.9761
Hexanal	66-25-1	1086	1084	56	A	98%	Sigma–Aldrich	A	Y = 1.3283 × X − 0.0314	0.9989
trans-2-Hexenal	6728-26-3	1230	1231	55	B			Hexanal	Y = 0.7147 × X + 0.0047	0.9986
Nonanal	124-19-6	1402	1402	57	A	95%	Sigma–Aldrich	A	Y = 2.0585 × X + 0.0018	0.9881
Heptanal	111-71-7	1189	1186	70	B			Nonanal	Y = 1.3283 × X − 0.0314	0.9989
trans-2-Heptenal	18829-55-5	1335	1336	83	B			Nonanal	Y = 1.3283 × X − 0.0314	0.9989
Decanal	112-31-2	1509	1506	57	B			Nonanal	Y = 1.3283 × X − 0.0315	0.9989
Hexanoic acid	142-62-1	1869	1869	60	A	99%	Sigma–Aldrich	A	Y = 1.5206 × X − 0.0363	0.9966
Ethyl butanoate	105-54-4	1041	1039	71	A	99%	Sigma–Aldrich	A	Y = 2.7781 × X − 0.001	0.9995
Butyl acetate	123-86-4	1077	1075	56	A	99%	Sigma–Aldrich	A	Y = 0.3517 × X − 0.1564	0.9957
Butyl propionate	590-01-2	1146	1145	57	A	99%	Sigma–Aldrich	A	Y = 0.2618 × X − 0.0856	0.9957
Butyl 2-propenoate	141-32-2	1185	1189	55	B			Butyl propionate	Y = 0.2618 × X − 0.0856	0.9957
Ethyl hexanoate	123-66-0	1242	1244	88	A	99%	Sigma–Aldrich	A	Y = 8.4587 × X + 0.0001	0.9994
Hexyl acetate	142-92-7	1279	1282	43	A	99%	Sigma–Aldrich	A	Y = 0.3564 × X − 0.1254	0.9957
Propyl octanoate	624-13-5	1526	1526	145	A	98%	Macklin	A	Y = 6.9526 × X + 0.0001	0.9996
γ-Butyrolactone	96-48-0	1654	1652	42	A	99%	Sigma–Aldrich	A	Y = 9.598 × X − 0.0131	0.9996
Guaiacol	90-05-1	1882	1884	109	A	99%	Sigma–Aldrich	A	Y = 0.9011 × X + 0.0001	0.9914
2-Methylphenol	95-48-7	2028	2030	108	A	99%	Sigma–Aldrich	A	Y = 1.2188 × X − 0.0007	0.9938
Phenol	108-95-2	2033	2032	94	A	99%	Sigma–Aldrich	A	Y = 1.2188 × X − 0.0007	0.9938
4-Ethyl guaiacol	2785-89-9	2052	2058	137	A	98%	Sigma–Aldrich	A	Y = 0.9001 × X − 0.0001	0.9914
3-Methylphenol	108-39-4	2113	2112	108	B			4-Methylphenol	Y = 1.2188 × X − 0.0007	0.9938
4-Methylphenol	106-44-5	2117	2121	108	A	99%	Sigma–Aldrich	A	Y = 1.2188 × X − 0.0007	0.9938
4-Ethylphenol	123-07-9	2200	2196	107	A	97%	Sigma–Aldrich	A	Y = 0.514 × X − 0.0001	0.9954
4-Vinylguaiacol	7786-61-0	2221	2217	150	A	98%	Sigma–Aldrich	A	Y = 0.9011 × X − 0.0001	0.9914
2,4-Di-*tert*-butylphenol	96-76-4	2328	2315	191	A	99%	Sigma–Aldrich	A	Y = 1.2188 × X − 0.0007	0.9938
4-Vinylphenol	2628-17-3	2420	2417	120	A	95%	J&K	A	Y = 0.8654 × X − 0.0004	0.9938

Table 1. *Cont.*

Compounds	CAS	RI Calculated	RI in Literatures	Quantitative Ion (*m*/*z*)	Identification *	Purity of Standards	Manufacturers of Standards	Quantitative Standards	Calibration Curves	R^2
Benzaldehyde	100-52-7	1546	1546	105	A	99%	Sigma–Aldrich	A	Y = 6.9511 × X − 0.0201	0.9964
4-Methylbenzaldehyde	104-87-0	1639	1638	120	B			Benzaldehyde	Y = 6.9511 × X − 0.0201	0.9964
Benzylethylaldehyde	122-78-1	1664	1662	91	A	95%	Sigma–Aldrich	A	Y = 0.937 × X − 0.0001	0.9877
3,5-Dimethylbenzaldehyde	5779-95-3	1836	1837	133	B			Benzaldehyde	Y = 6.9511 × X − 0.0201	0.9964
α-Phenylethanol	98-85-1	1830	1827	107	B			β-Phenylethanol	Y = 1.0633 × X − 0.052	0.9935
Benzyl alcohol	100-51-6	1897	1896	108	A	98%	Sigma–Aldrich	A	Y = 0.2772 × X − 0.0014	0.9980
β-Phenylethanol	1960/12/8	1933	1935	91	A	99%	Sigma–Aldrich	A	Y = 1.0633 × X − 0.052	0.9935
Styrene	100-42-5	1270	1267	104	A	99%	Sigma–Aldrich	A	Y = 1.3254 × X − 0.6542	0.9926
p-Cymene	99-87-6	1283	1278	119	B			Styrene	Y = 1.3254 × X − 0.6543	0.9926
Naphthalene	91-20-3	1764	1763	128	A	99%	Sigma–Aldrich	A	Y = 1.5624 × X − 0.3541	0.9859
2-Methylnaphthalene	91-57-6	1876	1872	142	B			Naphthalene	Y = 1.5624 × X − 0.3542	0.9859
Methyl salicylate	119-36-8	1798	1798	120	A	99%	Sigma–Aldrich	A	Y = 2.1954 × X − 0.0001	0.9967
2-Phenethyl acetate	103-45-7	1833	1835	104	A	99%	Sigma–Aldrich	A	Y = 0.0038 × X − 0.0001	0.9984
2-Methyl-1-propanol	78-83-1	1097	1097	43	A	99%	Sigma–Aldrich	A	Y = 0.1135 × X − 0.0016	0.9982
2-Methyl-1-butanol	137-32-6	1213	1208	57	A	98%	Sigma–Aldrich	A	Y = 0.6546 × X − 0.0125	0.9989
3-Methyl-1-butanol	123-51-3	1214	1210	55	A	98%	Sigma–Aldrich	A	Y = 0.4941 × X − 0.0014	0.9997
3-Methyl-2-butenol	556-82-1	1326	1327	71	B			3-Methyl-1-butanol	Y = 0.4941 × X − 0.0014	0.9997
4-Methyl-3-pentenol	763-89-3	1395	1390	69	B			*trans*-2-Hexenol	Y = 0.5711 × X − 0.0015	0.9998
3-Octanol	589-98-0	1397	1398	83	A	99%	Sigma–Aldrich	A	Y = 0.3196 × X − 0.0172	0.9991
2-Octanol	123-96-6	1422	1421	45	B			3-Octanol	Y = 0.3196 × X − 0.0172	0.9991
1-Octen-3-ol	3391-86-4	1457	1460	57	A	98%	Sigma–Aldrich	A	Y = 0.3844 × X − 0.0021	0.9994
2-Ethyl-1-hexanol	104-76-7	1496	1496	57	A	99%	Sigma–Aldrich	A	Y = 0.5869 × X − 0.0154	0.9966
trans-2-Heptenol	33467-76-4	1517	1517	57	B			Heptanol	Y = 0.3196 × X − 0.0172	0.9991
2-Nonanol	628-99-9	1522	1522	45	B			Octanol	Y = 0.0158 × X − 0.0001	0.9949
Isoamyl acetate	123-92-2	1130	1132	43	A	99%	Macklin	A	Y = 9.598 × X − 0.0131	0.9996
Ethyl 2-methylbutanoate	7452-79-1	1056	1056	102	A	99%	Sigma–Aldrich	A	Y = 2.7781 × X − 0.001	0.9995
2-Methylbutanal	96-17-3	920	920	57	B			Hexanal	Y = 1.3283 × X − 0.0314	0.9989
3-Methylbutanal	590-86-3	924	924	44	B			Hexanal	Y = 1.3283 × X − 0.0314	0.9989
β-Myrcene	123-35-3	1162	1167	93	B			Limonene	Y = 1.1804 × X − 0.0001	0.9947
α-Terpinene	99-86-5	1187	1183	121	A	95%	Sigma–Aldrich	A	Y = 0.9491 × X − 0.0001	0.9963
Limonene	138-86-3	1207	1195	68	A	96%	Sigma–Aldrich	A	Y = 1.1804 × X − 0.0001	0.9947
β-Phellandrene	555-10-2	1216	1218	93	B			Limonene	Y = 1.1804 × X − 0.0001	0.9947
β-*cis*-Ocimene	3338-55-4	1242	1252	93	B			Limonene	Y = 1.1804 × X − 0.0001	0.9947
β-trans-Ocimene	3779-61-1	1260	1260	93	B			Limonene	Y = 1.1804 × X − 0.0001	0.9947
α-Terpinolene	586-62-9	1291	1290	121	B			Limonene	Y = 1.1804 × X − 0.0001	0.9947
cis-Rose oxide	16409-43-1	1360	1363	139	A	99%	Sigma–Aldrich	A	Y = 0.0105 × X − 0.0001	0.9964
trans-Rose oxide	876-18-6	1376	1383	139	B			*cis*-Rose oxide	Y = 0.0105 × X − 0.0001	0.9964
cis-Allo-ocimene	673-84-7	1383	1382	121	B			Limonene	Y = 1.1804 × X − 0.0001	0.9947
trans-Allo-ocimene	14947-20-7	1404	1403	121	B			Limonene	Y = 1.1804 × X − 0.0001	0.9947
trans-Linalol furanoxide	34995-77-2	1451	1450	59	B			Linalool	Y = 0.0027 × X − 0.0001	0.9940
cis-Linalol furanoxide	5989-33-3	1481	1478	59	B			Linalool	Y = 0.0027 × X − 0.0001	0.9940

Table 1. *Cont.*

Compounds	CAS	RI Calculated	RI in Literatures	Quantitative Ion (*m*/*z*)	Identification *	Purity of Standards	Manufacturers of Standards	Quantitative Standards	Calibration Curves	R^2
Nerol oxide	1786-08-9	1482	1480	68	B			Nerol	$Y = 1.475 \times X - 0.0004$	0.9984
Linalool	78-70-6	1554	1554	93	A	97%	Sigma–Aldrich	A	$Y = 0.0027 \times X - 0.0001$	0.9940
Terpinen-4-ol	562-74-3	1615	1617	71	A	95%	Sigma–Aldrich	A	$Y = 0.0025 \times X - 0.0001$	0.9962
Hotrienol	29957-43-5	1619	1616	71	A			A	$Y = 0.0027 \times X - 0.0001$	0.9940
Neral	106-26-3	1698	1694	69	B			Nerol	$Y = 1.475 \times X - 0.0004$	0.9984
α-Terpineol	98-55-5	1709	1707	59	A	96%	Sigma–Aldrich	A	$Y = 0.0025 \times X - 0.0001$	0.9962
Citral	5392-40-5	1748	1733	69	B			Nerol	$Y = 1.475 \times X - 0.0004$	0.9984
trans-Pyran linalool oxide	39028-58-5	1752	1749	68	B			Linalool	$Y = 0.0027 \times X - 0.0001$	0.9940
Citronellol	106-22-9	1774	1772	69	A	95%	Sigma–Aldrich	A	$Y = 0.0026 \times X - 0.0001$	0.9969
γ-Isogeraniol	13066-51-8	1797	1800	69	B			Geraniol	$Y = 0.9871 \times X - 0.0004$	0.9980
Nerol	106-25-2	1810	1808	69	A	97%	Sigma–Aldrich	A	$Y = 1.475 \times X - 0.0004$	0.9984
Geraniol	106-24-1	1856	1857	69	A	99%	Sigma–Aldrich	A	$Y = 0.9871 \times X - 0.0004$	0.9980
6-Methyl-5-hepten-2-one	110-93-0	1347	1345	108	B			Nonanal	$Y = 2.0585 \times X + 0.0018$	0.9881
6-Methyl-5-hepten-2-ol	1569-60-4	1469	1467	95	B			Octanol	$Y = 0.3196 \times X - 0.0172$	0.9991
α-Cyclogeraniol	6627-74-3	1715	NA	123	C			β-Damascenone	$Y = 0.0057 \times X - 0.0001$	0.9990
β-Damascenone	23726-93-4	1837	1838	69	A	98%	Macklin	A	$Y = 0.0057 \times X - 0.0001$	0.9990
2-Pentylfuran	3777-69-3	1240	1244	81	B			Furfural	$Y = 0.846 \times X - 0.0041$	0.9985
Furfural	98-01-1	1482	1482	96	A	99%	Sigma–Aldrich	A	$Y = 0.846 \times X - 0.0041$	0.9985

*: "A" means the compound was identified by the standard; "B" means the compound was identified by the RI from the literature; "C" means the compound was identified by the NIST library. **: "A" means quantified by the corresponding standard. CAS: CAS registry number; RI: retention index; R^2: coefficient of determination.

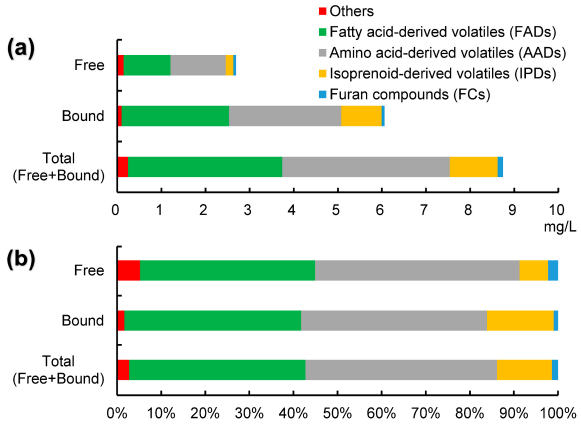

Figure 2. Concentration (**a**) and percentage (**b**) of volatile compounds in Vidal grapes at harvest (T5).

3.2.1. FADs

The percentage of FADs in the total content (free + bound) of volatile compounds in Vidal grapes (T5) was 39.97%, and their percentage in free and bound forms of volatiles was 39.67% and 40.10%, respectively (Figure 2). The FADs were present mainly in glycosidically bound form, being 2.27 times higher than those in free form. Twenty-seven FADs were detected in Vidal grapes, including 12 straight-chain alcohols, 6 straight-chain aldehydes, 1 straight-chain acid, 7 straight-chain esters, and 1 lactone. Straight-chain alcohols and aldehydes were the two most abundant compounds, accounting for 95.82% of the total FADs. The C6/C9 alcohols and aldehydes derived from the enzymatic oxidation of fatty acids through the lipoxygenase pathway are the main constituents of this group of compounds, which are the main source of 'green' or 'herbaceous' odors in grape juice and wine [2]. Among the free-form volatile compounds, the most abundant FADs were butanol, hexanol, hexanal, and *trans*-2-hexenol, which accounted for 18.58%, 14.89%, 12.19%, and 11.60% of the FDAs, respectively. Yet, within the bound forms, the largest contents were observed for nonanol, butanol, *cis*-6-nonenol, and hexanol, with percentages of 46.16%, 13.41%, 11.79%, and 9.66%, respectively. Unlike the high level of C6 aldehydes in grapes harvested at regular maturity [2,3], the content of hexanal in on-vine dehydrated Vidal grapes was not the highest of FADs, representing only 5.29% of the total FADs and much lower than the contents of nonanol and butanol, which accounted for 34.57% and 14.99% of the total FADs, respectively. In the study conducted by Genovese et al. (2007) [9], it has also been found that butanol was one of the characteristic odorants distinguishing sweet Fiano wine from base Fiano wine, the former being made from dehydrated grapes while the latter was made from grapes at normal maturity.

3.2.2. AADs

The AADs were the most abundant and most diverse in both free and bound forms, including 23 benzenoids (or phenylpropanoids) and 15 branched-chain aliphatics. The benzenoids content accounted for 76.79% of the total AADs, which are generated by the metabolism of phenylalanine [4,27], while the branched-chain aliphatics are derived from the metabolism of branched-chain amino acids such as valine, leucine, and isoleucine [4], including some branched-chain alcohols, aldehydes, and esters.

Considering the contribution to the final dessert wine aroma, volatile phenols seem to play a greater role in AADs from grapes, as branched-chain aliphatics and most other phenylpropanoids were present in much lower amounts in grape berries than those produced by yeast during alcoholic fermentation [4]. A total of 10 volatile phenols were identified in Vidal grapes (T5), and 98.62% of the total content was present in glycosidically bound forms, indicating the great potential contribution to the dried fruit and caramel note of the resulting wine [4,11]. Some authors have also observed higher and increased contents of bound volatile phenols in Garnacha Tintorera grapes during artificial post-harvest

drying [11]. Based on our data, guaiacol and 4-vinylguaiacol, with a low threshold (1 μg/L and 3 μg/L in water [28], respectively) and smoky, sweet, phenolic, and spicy flavors, can be considered the most valuable compounds of this group in Vidal grapes.

With the aromatic characteristics of honey and rose, benzylethylaldehyde and 2-phenethyl acetate are two other crucial odorants of phenyl derivatives in Vidal grapes, whose thresholds were detected at 4 μg/L and 250 μg/L in water [28], respectively. Phenylacetaldehyde was present mainly in the free form, which was 10.70 times higher than the bound form, and exceeded its threshold by 20 times. Although the free form of 2-phenethyl acetate was lower than its threshold, its total content was 2.78 times higher than its threshold. Besides phenylacetaldehyde, two important Strecker aldehydes, namely, 2-methylbutanal and 3-methylbutanal (isovaleraldehyde), were also detected at considerably high levels in Vidal grapes at T5. These two compounds were presented completely in free forms in the grapes, with concentration above 50 μg/L. Characterized by malt, cocoa, and almond aromas with extremely low thresholds (less than 1 μg/L) and strong synergistic effects [29], 2-methylbutanal and 3-methylbutanal might contribute directly to the wine aroma.

3.2.3. IPDs

The percentage of IPDs in the total content of volatile compounds was 12.45%, where the percentages of free and bound forms of volatiles were 6.33% and 15.18%, respectively (Figure 2). Twenty-five monoterpenoids and four norisoprenoids were detected in Vidal grapes, whose percentages in the total IPDs were 99.33% and 0.67%, respectively. The IPDs were present mainly in glycosidically bound form, which was 5.41 times higher than the free form, accounting for 84.40% of the total IPDs.

Among the monoterpenes, the most abundant were geraniol, linalool, β-*trans*-ocimene, and β-myrcene, which accounted for 62.14% of the total monoterpene content (free + bound) at 30.52%, 10.24%, 11.06%, and 10.32%, respectively. Similar to Muscat varieties [2], linalool and geraniol were the most important monoterpenes in Vidal grapes from the Weixi region, where both concentrations of free forms were above their odor threshold. The total content of free and bound forms of linalool and geraniol reached 18.51 and 8.27 times their thresholds, respectively, which means that they would contribute directly to the final wine aroma, with hyacinth, rose, and citrus notes [2]. Although *cis*-rose oxide was not present in high concentrations, it is another powerful aromatic compound for Vidal grapes, due to its low threshold (0.1–0.5 μg/L), as described in Gewurztraminer, Muscat, Traminette, and Riesling grapes [2,28].

Four norisoprenoids were detected in Vidal grapes, of which β-damascenone was undoubtedly the most essential. Contrary to most terpenes, the free form of β-damascenone was 5.93 times more than that of the bound form—a level that is 58.80 times its threshold in water (0.01 μg/L [29]). Some authors have also found that β-damascenone accumulated during the late-harvest dehydration process of Shiraz grapes [30] and the storing process of raisins [15].

3.3. Evolution of the Volatile Compounds during Dehydration

In order to intuitively visualize the evolution pattern of volatile compounds during on-vine grape dehydration, their contents (expressed as μg/L and ng/berry) were analyzed by hierarchical clustering, and the results are presented as heatmaps in Figure 3a,b. In the heat maps, each column corresponds to a dehydration degree (T1, T2, T3, T4, and T5), each row represents a compound, and each cell color reflects the content level of the compound, where red indicates a high content level and blue indicates a low level. As the columns are arranged according to the time sequence of sampling, the color variation in each row reflects the evolution of a compound during the dehydration process. All volatiles were hierarchically clustered based on their evolution pattern, and are illustrated in the dendrogram on the left of each heatmap.

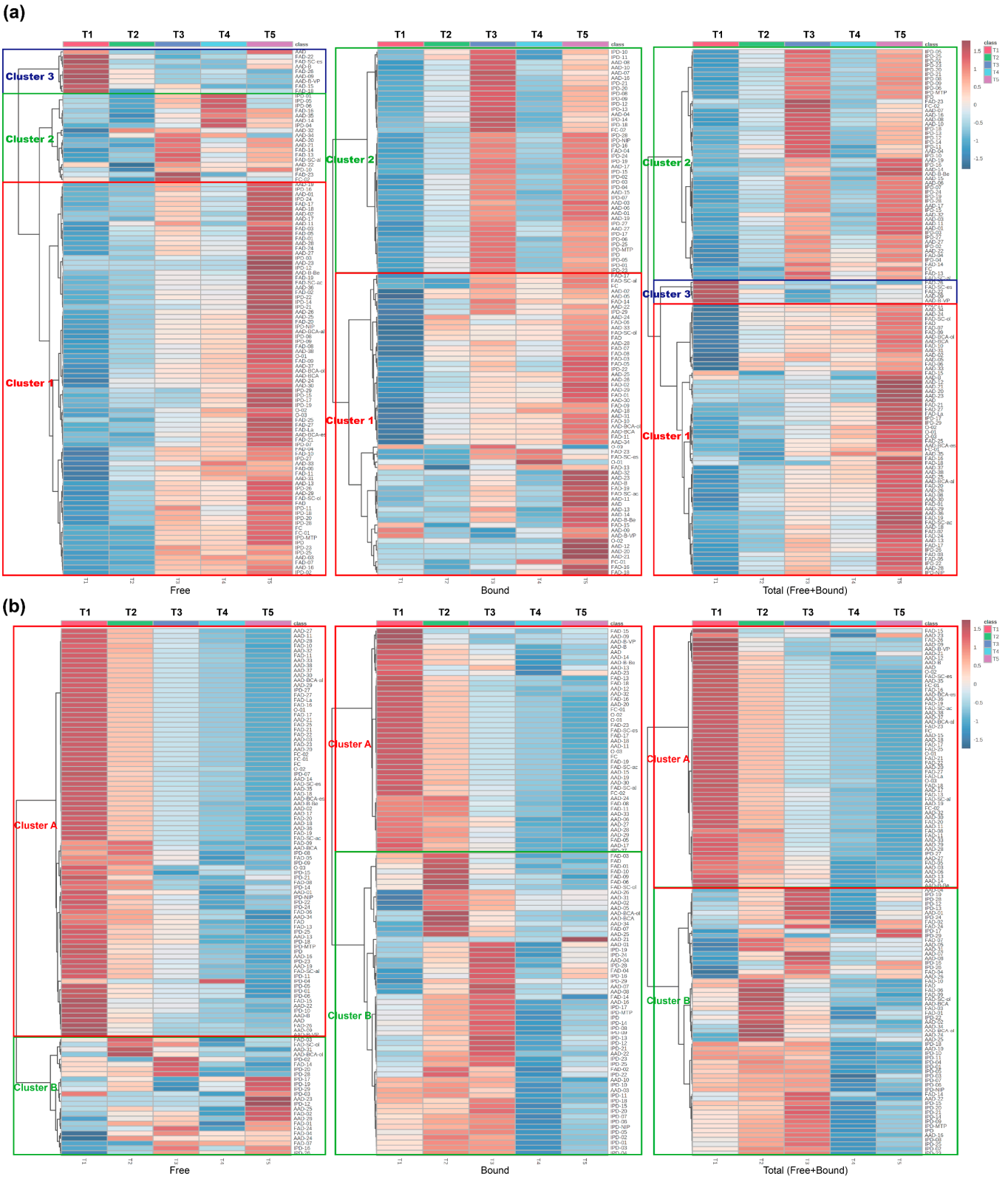

Figure 3. Hierarchical cluster heatmaps of free, bound, and total volatile compounds expressed by μg/L in grape juice (**a**) and ng/berry in every single berry (**b**). The corresponding compounds for the abbreviations are listed in Tables S1 and S2. T1, T2, T3, T4, and T5 represent the sampling points at different dehydration degrees.

To the best of our knowledge, few studies have investigated the evolution of volatiles during grape dehydration using the two expressions of μg/L and ng/berry simultaneously. The heatmaps indicated that the evolution patterns of volatile compounds were completely different, according to these two compound content expressions.

3.3.1. Volatile Compounds Evolution Expressed as μg/L

From an enological point of view, the content of grape volatiles expressed as μg/L could directly correlate to the wine composition, which is why many studies have used this unit to calculate their results. The influence of dehydration degree on grape volatiles could also reflect, to some extent, its effect on the final wine aroma. The evolutions of free, bound, and total (free + bound) volatile compounds are illustrated in the heatmaps in Figure 3a.

According to the hierarchical clustering results, we divided the evolution of all volatiles during dehydration into three clusters. Cluster 1 gradually increased during dehydration and reached a peak at T5. Cluster 2 fluctuated and reached its maximum value between T3 and T5. Cluster 3 was highest at the beginning of dehydration and gradually decreased during the process. The clustering categorization of the volatiles is listed in Table S1. Generally speaking, most of the volatile compounds increased during the on-vine grape dehydration process, with only a few decreasing.

FADs: Eighteen FADs were classified into Cluster 1 in both the free and bound forms, six FADs were classified into Cluster 2 in either the free or bound forms, four FADs were classified as Cluster 3 in free forms, and no bound forms of FADs were classified into Cluster 3. For the total FADs (free + bound), twenty compounds were classified into Cluster 1, four compounds were classified into Cluster 2, and only two esters (butyl propionate, propyl octanoate) were classified into Cluster 3. Among the most important C6/C9 compounds of FADs, nine of them were classified as Cluster 1 in both the free and bound forms, while only four were classified into Cluster 2 or Cluster 3. The bound forms of *trans*-2-hexenol, as well as the free forms of hexanal and *trans*-2-hexenal were all classified into Cluster 2, with fluctuating levels during berry dehydration and reaching a maximum at T3 or T4. Considering the impact on sensory quality, the evolution of some critical C6 compounds during the dehydration process is shown in Figure 4a. With typical grassy notes, hexanal was present at levels above its thresholds at different levels of dehydration. Dehydration promoted an increase in *trans*-2-hexenal content and exceeded the threshold after T2, with a small decrease after peaking at T3.

AADs: Twenty-two free forms and twenty-three bound forms of AADs were grouped into Cluster 1, including twelve compounds with both forms classified in this group. Seven free forms and twelve bound forms AADs were grouped into Cluster 2. Only the free form of one compound (2,4-di-*tert*-butylphenol) was grouped into Class 3. In Cluster 2, the majority (sixteen compounds) were phenylpropanoids in free or bound forms, and only four compounds belonged to the branched-chain aliphatics. The fluctuating variation in phenylpropanoids—especially the bound forms of volatile phenols—during on-vine berry dehydration indicated that water-loss enrichment was not the only affecting factor in this process. Interestingly, the content of 2-phenethyl acetate, with rose and honey notes, was dramatically increased at the late stage of dehydration (T5), reaching 2.79 times its threshold (Figure 5a). Another powerful floral composition with a low threshold was phenylethylaldehyde, the free form content of which increased gradually throughout the water-loss process.

IPDs: Most of the free forms of IPDs (24 compounds) were classified into Cluster 1, except for five kinds of monoterpenes, namely, β-myrcene, β-phellandrene, β-*cis*-Ocimene, β-*trans*-Ocimene, and *cis*-allo-ocimene. In contrast, all the bound fractions of IPDs were grouped into Cluster 2, except for citronellol and β-damascenone. Undoubtedly, as the bound fraction was the main form of IPDs (Figures 2a and 6), the total content (free + bound) of IPDs was also mainly classified into Cluster 2, except for hotrienol, citronellol, 6-methyl-5-hepten-2-one, and β-damascenone. The evolution of some organoleptic key monoterpenoids and norisoprenoids is plotted in Figure 6a. Although the content of the bound

forms of β-myrcene, linalool, and geraniol fluctuated during the late stages of grape dehydration, they were all considerably increased at T5 compared to T1. However, the increase in the free forms during this process was more limited, except for the *cis*- or *trans*- rose oxide, whose free state increased steadily during dehydration. Dominated by the free fractions, β-damascenone showed a different trend from monoterpenoids, with the free forms increasing far more sharply than the bound forms from T1 to T5, especially after T3.

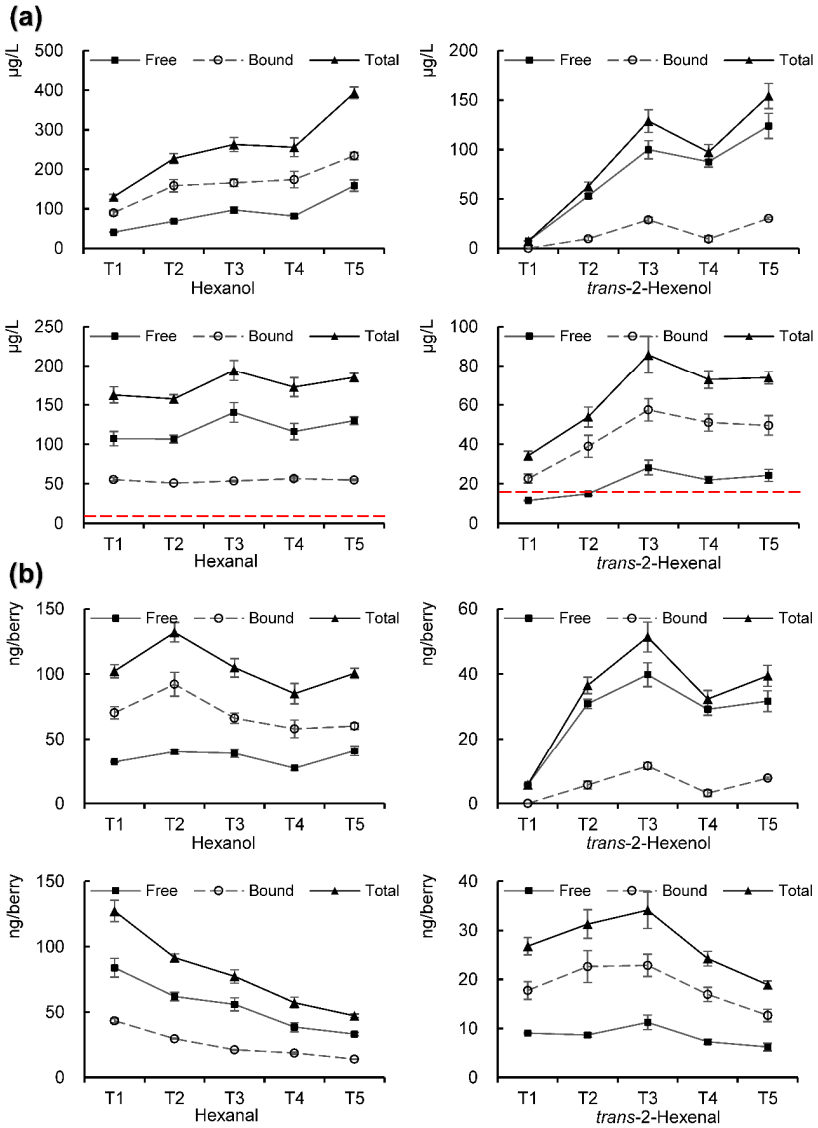

Figure 4. Evolution of some C6 compounds during on-vine grape dehydration. The red dashed line marks the threshold level: (**a**) μg/L; (**b**) ng/berry. T1, T2, T3, T4, and T5 represent the sampling points at different dehydration degrees. Values are the means of three replicates. The error bars represent the standard deviation.

In general, the results of hierarchical clustering for volatiles expressed as μg/L in grape juice indicated that the vast majority of the free and bound fractions (Clusters 1 and 2) were finally enhanced by on-vine dehydration, except for some FADs (Cluster 3), such as nonanal, decanal, butyl propionate, and propyl octanoate. It should be noted that most of the bound forms of terpenes and volatile phenols (Cluster 2) showed complex fluctuating changes during the on-vine dehydration process, indicating that these compounds were not only enhanced by the water loss-induced inspissation, but also reduced by other mechanisms.

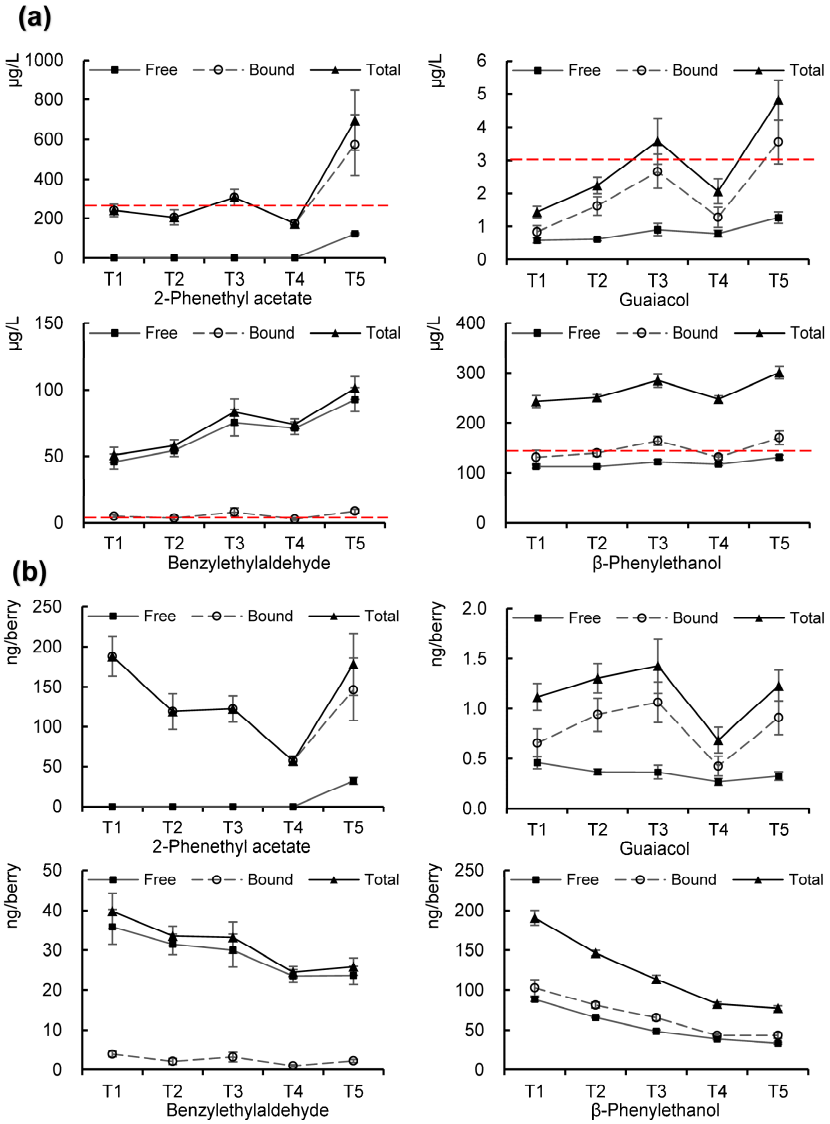

Figure 5. The evolution of some phenylpropanoids during on-vine grape dehydration. The red dashed line marks the threshold level: (**a**) μg/L; (**b**) ng/berry. T1, T2, T3, T4, and T5 represent the sampling points at different dehydration degrees. Values are the means of three replicates. The error bars represent the standard deviation.

3.3.2. Volatile Compounds Evolution Expressed as ng/berry

To further elucidate the evolution pattern of overall volatiles in each grape berry during on-vine dehydration, ng/berry expression was employed as a measurement unit for the calculation of volatile content. The resulting dataset was also processed for hierarchical clustering heatmap analysis. We expected that some useful information on the biochemical metabolism of volatiles during on-vine dehydration could be obtained in this way.

The evolutions of the free, bound, and total (free + bound) volatile compounds in a single berry are visualized in the heatmaps in Figure 3b. All volatiles were grouped into two clusters through hierarchical clustering. In Cluster A, the volatiles gradually decreased throughout the dehydration process. In Cluster B, volatiles fluctuated during dehydration and peaked at some stage after T1. The cluster information of volatiles is listed in Table S2. According to the heatmaps shown in Figure 3, the tendency of volatiles during dehydration calculated in ng/berry presented a completely different pattern than that in ug/L. For a single grape berry, most of the volatiles were reduced by the biochemical process substantially at the end of grape dehydration (T5), except for a few IPDs in free

forms. During the on-vine dehydration process, the volatiles showed a complex variation trend under the combined action of two opposite effects, namely, biodegradation and water-loss concentration. This finding provides a good explanation for the content fluctuations of some volatiles during on-vine dehydration in this study, as well as in those conducted by others [13,19,31].

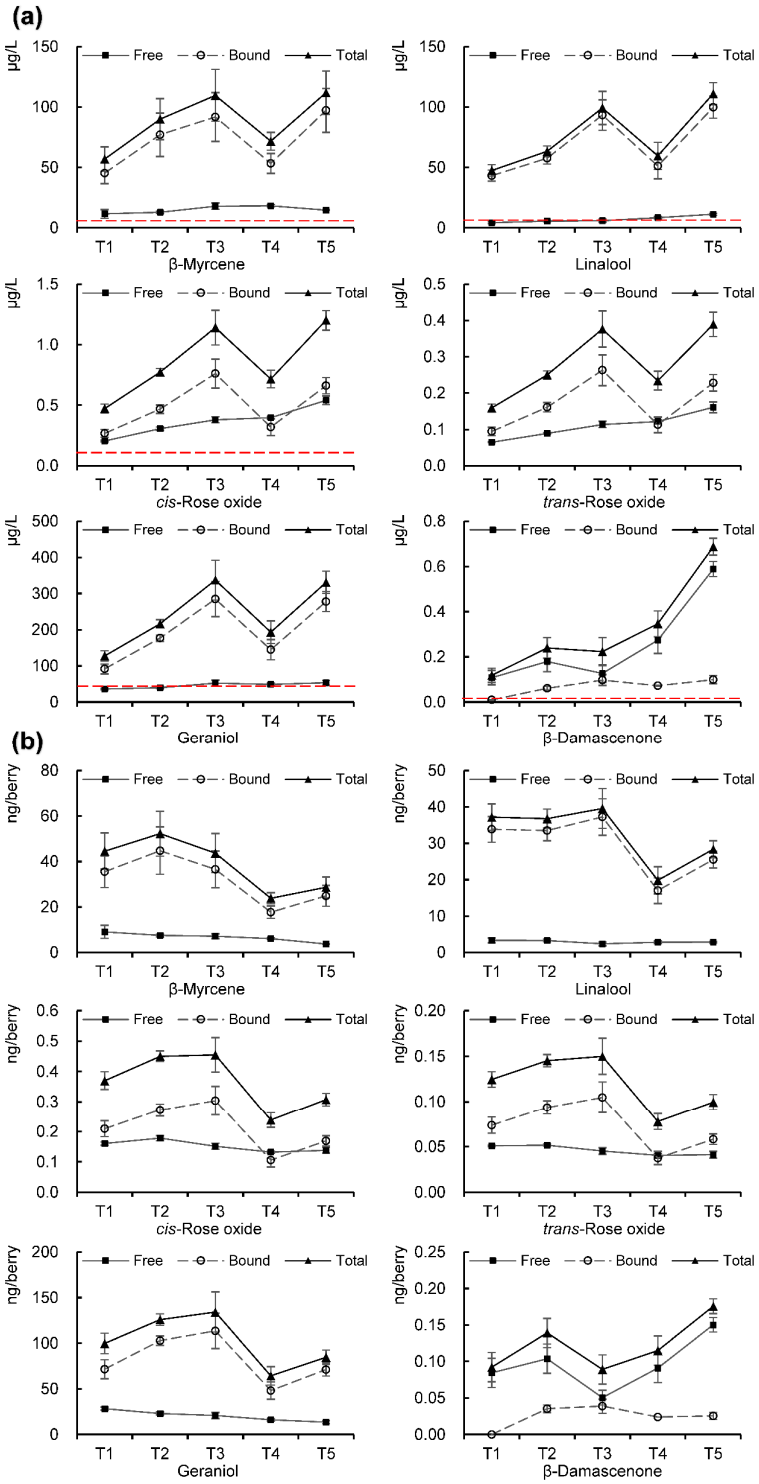

Figure 6. Evolution of some IPDs during on-vine grape dehydration. The red dashed line marks the threshold level: (**a**) μg/L; (**b**) ng/berry. T1, T2, T3, T4, and T5 represent the sampling points at different dehydration degrees. Values are the means of three replicates. The error bars represent the standard deviation.

FADs: With the exception of *trans*-2-hexenal and ethyl hexanoate, most of the straight-chain aldehydes and esters derived from fatty acids (Cluster A) gradually decreased after T1. Some key C6 compounds (Figure 4b) were classified into Cluster B in both the free and bound forms, including hexanol, *trans*-3-hexenol, *cis*-3-hexenol, *trans*-2-hexenol, and *trans*-2-hexenal. Both free and bound forms of hexanal gradually decreased at almost the same rate throughout the dehydration process, and the total content (free + bound) at T5 was only 37.13% that at T1. Due to the water-loss concentration effect, the content of hexanal presented in grape juice (μg/L) remained relatively constant during the whole dehydration process (Figure 4a). The contents of hexanol, *trans*-2-hexenol, and *trans*-2-hexenal increased at the early stage of dehydration and reached a peak at T2 or T3, and then decreased at different levels. It is worth noting that *trans*-2-hexenol was increased considerably in the early stage of dehydration, reaching a peak at T3, being 6.83 times higher than that at T1. A remarkable increase in glycosidically bound C6 alcohols and a consecutive decrease in C6 aldehydes (ng/berry) has also being observed in the on-vine dehydration of Beibinghong grapes for icewine-making in the northeast of China [19]. A similar phenomenon during an off-vine artificial grape-drying process has also been noted by other authors, with a continuous decrease in C6 aldehydes and a previous increase followed by a subsequent decrease in C6 alcohols. [11]. The variation in C6 compounds during grape dehydration is probably due to lipoxygenase (LOX) activity changes in response to the water stress caused by dehydration and the reactions between the aldehydes and grape polyphenols [2,26].

AADs: The majority of free AADs were classified into Cluster A, except for 2-phenethyl acetate, 2-methyl-1-propanol, 2-methyl-1-butanol, 3-methyl-1-butanol, and 1-octen-3-ol, all of which were classified as Cluster B. For the bound fractions of AADs, twenty-three compounds were assigned into Cluster A, while fifteen compounds (dominated by 11 phenylpropanoids) were assigned into Cluster B. Volatile phenols were found mainly in the bound forms, all of which were classified into Cluster B, except for 4-methylphenol and 2,4-di-*tert*-butylphenol. Taking guaiacol as an example, the free forms decreased slightly during the dehydration process, while the bound forms fluctuated in the later stages of this process (Figure 5b). 2-Phenethyl acetate, characterized by a pleasant rose and honey aroma, decreased rapidly in the early stages of dehydration, but significantly increased in the later stages of dehydration, where the berry weight loss exceeded 30% (T4). Consequently, its content in the juice (μg/L) rapidly exceeded its threshold at T5 under the combined effect of the dehydration concentration and biosynthesis through some unknown mechanism(s) (see Figure 5). Two other important floral compounds, phenylethylaldehyde and β-phenylethanol, were gradually degraded during the dehydration process, but their content in grape juice (μg/L) did not decline, as the concentration effect of dehydration was greater than the degradation effect (Figure 5). It should be emphasized that the levels of the mushroom-like odorant 1-octen-3-ol—a typical molecular marker of *Botrytis cinerea* or other fungal infections [21,32–34]—did not increase notably throughout the dehydration process (Table S2), indicating that the grapes in this study was not infected by such pathogens during dehydration.

IPDs: Nineteen free IPDs were grouped into Cluster A, with a gradual decrease after T1, and another ten free IPDs were grouped into Cluster B, with fluctuating changes during the same process. The evolutions of bound and total IPDs were relatively complex, all of which were classified into Cluster B, except 6-methyl-5-hepten-2-ol. With a continuous decrease in the free fractions, the predominately glycosidically bound forms of five key monoterpenoids showed different variation trends during the dehydration process (Figure 6b). They increased in the early stages of dehydration and then decreased significantly, followed by a clear rebound at T5. Progressive decreases in free monoterpenoids during on-vine dehydration have also been observed by various authors in different grape varieties, such as Beibinghong [19], Aleatico [35], and Moscato bianco [10,35,36]. Several recent studies have focused on the evolution patterns of glycosidic precursors during grape ripening, some of which found no significant changes [11] or slight increases [23] in terpenoids during dehydration, while others observed dramatic decreases [35]. The incon-

sistent results of these studies suggest that the accumulation patterns of monoterpenoids are greatly influenced by multiple factors, such as the volatiles themself [37], grape variety [38], and vintage [39], making it difficult to draw a simple conclusion. D'Onofrio et al. (2013) have pointed out that the different evolution patterns of aromatic compounds during late-harvest drying in different regions and vintages suggest that the content variations of volatiles are largely determined by environmental factors [10].

Different from C6 compounds (Figure 4b), the free and bound forms of terpenoids evolved in a completely different pattern during the dehydration process in our study (Figure 6b). An increase in glycosylated terpenoids and decrease in free forms caused by water loss have also been observed by other authors [36]. We presume that this might be caused by the conversion of free terpenoids to bound forms under the catalyzation of glycosyltransferase during the dehydration process. As the dehydration concentration leads to high sugar levels and high hydrophilicity in the vacuolar, the cells need to convert the hydrophobic free forms of terpenoids with increasing content (μg/L) to their hydrophilic glycosidically bound forms in order to avoid their crossing the tonoplast and reducing their toxicity [1]. Of course, further studies are needed to support this hypothesis.

The evolution of β-damascenone—the most potent aromatic C13-norisoprenoids with fruity and floral notes—differed from that of the terpenoids, indicating a distinct biosynthetic pathway [1,40]. In contrast to terpenoids, which exist mainly in the glycosidically bound form, the free form of β-damascenone was much more abundant than its bound form (Figure 6). The bound form of β-damascenone gradually increased in the early stages of dehydration, and then slightly decreased after peaking at T3. The free form of β-damascenone showed fluctuating changes in the early stages of dehydration but gradually increased steadily after T3. The total content of β-damascenone at T5 reached 1.91 times that at T1. Combined with the concentration effect caused by dehydration, its content in juice (μg/L) increased sharply in the late stages of dehydration, providing the molecular foundation for the complex floral and fruity characters in the final dessert wine. As has been demonstrated in other studies, β-damascenone is a key contributor to the aroma of icewine [21], noble-rotted wine [32], and late-harvest wine [9]. However, Lan et al. (2016) have found that free β-damascenone peaked in the middle of the late-harvest icing process (TM + 40 or TM + 50) in Beibinghong grapes, after which the content (ug/berry) gradually decreased [19]. They suggested that this change in β-damascenone was related to the regulation of *Vv*CCD1 and its biotransformation in the final stage. Before this, Cirilli et al. (2012) have observed that the expression of *Vv*CCD1 in off-vine drying Aleatico grapes was regulated by the dehydration degree and drying temperature [16]. A decrease in β-damascenone at the final stage of Vidal icewine grapes has also been reported by other authors [31].

We believe that the opposite tendency of β-damascenone in the last stage of late-harvest in our study, compared to that in the studies of Lan [19] and Chen [31], was due to the complete difference in berry structure at this stage. In their study, the grape cell structure was repeatedly damaged by freeze–thaw cycles, exposing the volatiles to an oxidative environment [19]. In contrast, the grapes in our study were not frozen during the dehydration process (Figure S1a, with the lowest temperature of −2.6 °C on 2 December); therefore, the cell structure and biochemical function remained intact and non-destructive, keeping the volatiles away from oxygen. Furthermore, their studies were conducted in northeastern China, where temperatures were extremely low during the later stage, whereas ours was in the southwest, at a lower latitude, with abundant sunlight and heat during the daytime throughout the dehydration period. As sunlight is positively correlated with an increase in β-damascenone [41], the biosynthesis of this compound might have been still progressing at the later dehydration stage in our study.

3.4. Screening of Volatiles Mainly Effected by Dehydration Concentration

In order to examine the relationship between the dehydration degree and the contents of volatiles, as well as to further screen the volatile compounds with content directly

determined by the dehydration concentration effect, unary linear regression analysis (U-LRA) was employed between the juice volumes per 100 berries (JV100) (Figure 1f) and the contents of volatiles, expressed as μg/L; the former was chosen as the independent variable and the latter was chosen as the dependent variable. The compounds with both $R^2 > 0.9$ and *p*-value of significance <0.01 are listed in Table 2. It should be noted that the JV100 directly represents the exact dehydration degree and concentration effect, with a lower JV100 indicating greater dehydration and concentration effect. Therefore, a negative correlation with the JV100 indicates a positive correlation with the dehydration degree.

Table 2. Results of the unary linear regression analysis (U-LRA) between juice volume per 100 berries (JV100) and volatile contents (μg/L).

	Free			Bound			Total		
	R^2	*p*-Value	RC *	R^2	*p*-Value	RC	R^2	*p*-Value	RC
trans-2-Hexenol	0.954	0.004	−2.087						
Pentanol							0.945	0.006	−0.519
Heptanol	0.982	0.001	−0.017						
Octanol	0.996	0.003	−0.004						
trans-2-Heptenal				0.943	0.006	−0.009			
Propyl octanoate	0.923	0.009	0.050	- **	-	-	0.923	0.009	0.050
Benzyl alcohol	0.980	0.001	−0.551						
Methyl salicylate				0.934	0.007	−0.031	0.935	0.007	−0.031
2-Methyl-1-butanol				0.963	0.003	−0.834	0.923	0.009	−1.450
3-Methyl-1-butanol				0.960	0.003	−1.231			
1-Octen-3-ol	**0.967**	**0.003**	**−0.011**	**0.943**	**0.006**	**−0.075**	**0.947**	**0.005**	**−0.086**
2-Methylbutanal	0.962	0.003	−0.055	-	-	-	0.962	0.003	−0.055
α-Terpinene	0.963	0.003	−0.048						

*: Regression coefficient. **: Not detected in this form.

The U-LRA results indicated that thirteen compounds expressed as μg/L were highly correlated with JV100 ($R^2 > 0.9$ and $p < 0.01$), twelve of which were negative and one positive. Six compounds in the free fraction were highly negatively correlated with JV100, namely, *trans*-2-hexenol, heptanol, octanol, benzyl alcohol, 1-octen-3-ol, 2-methylbutanal, and α-terpinene. For the bound fraction, *trans*-2-heptenal, methyl salicylate, 2-methyl-1-butanol, 3-methyl-1-butanol, and 1-octen-3-ol were highly negatively correlated with JV100. Regarding the total content of the free and bound forms, five compounds were highly negatively correlated with JV100, including pentanol, methyl salicylate, 2-methyl-1-butanol, 1-octen-3-ol, and 2-methylbutanal. The results of U-LRA indicated that the increases in these volatiles were mainly caused by the concentration effect, and these compounds remained relatively stable during the non-destructive on-vine dehydration process, especially 1-octen-3-ol. The free and bound forms, as well as the total content, of 1-octen-3-ol were highly negatively correlated with JV100. Although 1-octen-3-ol—a biochemical marker of fungal infection with a mushroom note—is a key aroma component in icewines and noble-rot wines, it can also impart off-flavors to the wine when present at high levels [33,42]. Therefore, the accumulation of this compound during the late-harvest process should be carefully monitored.

Propyl octanoate, which exists only in free form, was positively correlated with JV100, and its content decreased gradually despite the dehydration concentration effect, indicating that the degradation of this compound was faster than the concentration and was determined by the dehydration level.

3.5. Identification of Key Parameters at Different Dehydration Degree

Principal component analysis (PCA), an unsupervised multivariate statistical analysis method, was applied to examine the sample variance and clustering related to the dehydration degree. The PCA score scatter plots of the free and bound forms of volatiles, expressed as ng/berry, are shown in Figure S3. All samples were observed to be located

inside the 95% confidence interval after Hotelling's T2 investigation for the possibility of outliers. For the free fractions, the first two principal components (PCs) explained 86.5% and 12.8% of the overall variance, respectively. The score plot showed a clear separation of T1 from others. Although T2 could be distinguished from T3, T4, and T5 on PC1, the distance between them was much smaller than that of T1. However, T3, T4, and T5 could not be separated completely, in terms of either PC1 or PC2. For the bound fractions, PC1 and PC2 explained 95.0% and 3.5% of the overall variance, respectively. Similar to the PCA result of the free forms, T4 and T5 could not be separated visibly from each other on the score scatter plot of the bound forms. From the results above, it was difficult to find discriminative information for the metabolites between the five dehydration stages by PCA.

In order to obtain better discrimination and to further identify the marker metabolites of the different dehydration degrees, the supervised multivariate statistical analysis method of orthogonal partial least-squares discriminant analysis (OPLS-DA) was employed on both free and bound volatiles at different dehydration stages. OPLS-DA (also known as the orthogonal projection to latent structures discriminant analysis in some studies) has been widely used for classification or discrimination in metabolomics [43,44]. In this study, OPLS was used to develop discriminative analysis models for the free and bound fractions, respectively. The score scatter plots of these two models, shown in Figure 7a,b, illustrated that the OPLS model developed for the free forms of volatiles was a better fit than that of the bound forms, in terms of the discrimination of samples with respect to different dehydration degrees. The samples at the five dehydration stages were well-separated in the former model constructed from the free fractions, while samples were not discriminated well by the later model developed from the bound volatiles. Therefore, the former model was selected for further application in extracting information on marker metabolites at different dehydration degrees.

The discrimination model of free fractions was built after the observation classes were set according to the sampling point and the variables were scaled using the 'Par' scaling type. Four predictive components were achieved in the model with high cross-validation parameters, as follows: R2X(cum) = 0.996, R2Y(cum) = 0.992, and Q2(cum) = 0.965. High R2 and Q2 values indicate a good descriptive ability and predictability of the model [44]. A permutation test involving 200 runs was also applied, in order to observe the overfitting phenomenon of the model. With all intercepts of the Q2 regression line below zero, the permutation plots (shown in Supplementary Figure S4) indicated that the overfitting phenomenon did not exist; thus, the model was reliable. Consequently, the statistical model established for the free forms of volatiles expressed as ng/berry was employed to identify the key parameters caused by differing dehydration degree. For this purpose, the variable importance in projection (VIP) value was used to estimate the contribution of a given compound to the OPLS-DA model. Referring to SIMCA guidelines and other studies [45–48], the importance of a variable to the discriminant model was determined according to its VIP value, where the larger the VIP value, the more critical the compound is in the discriminant analysis. In general, compounds with VIP values above 1.0 can be considered as metabolic markers with strong contributions to the discriminant model. This screening criterion has also been set to 2.0 by some authors [48].

As shown in the VIP plot in Figure 7c, a total of twenty-seven free-form compounds with VIP values greater than 1.0 were screened as metabolic markers to discriminate the grapes at five degrees of on-vine dehydration. These differential metabolic markers consisted predominantly of ADDs and FADs, with thirteen ADDs and eleven FADs, while the only IPD was geraniol (with a VIP value of 1.03).

To visually elucidate the relationship between these metabolic markers and the five degrees of dehydration, hierarchical clustering heatmap analysis was conducted in MetaboAnalyst 5.0, with the samples and compounds clustered separately. After hierarchical clustering, the twenty-seven metabolic markers were divided into three clusters that each showed a different evolutionary pattern during dehydration. As shown in Figure 8,

Cluster I included a total of twenty compounds that gradually decreased during dehydration; Cluster II contained three compounds, whose content fluctuated during dehydration; and Cluster III contained five compounds, whose content increased significantly in the later stages of dehydration. Remarkably, the samples were also clustered in order of dehydration degree, indicating that the screened metabolic markers were able to discriminate the degree of dehydration very well. Four free-form volatiles with VIP values above 2.0 were the most important metabolic markers for discriminating the dehydration degree, namely, 2,4-di-*tert*-butylphenol (ADD09, in Cluster I, VIP = 4.34), 2-phenethyl acetate (ADD23, in Cluster III, VIP = 2.65), 2-methyl-1-propanol (ADD24, in Cluster II, VIP = 2.10), and hexanol (FAD01, in Cluster II, VIP = 2.08).

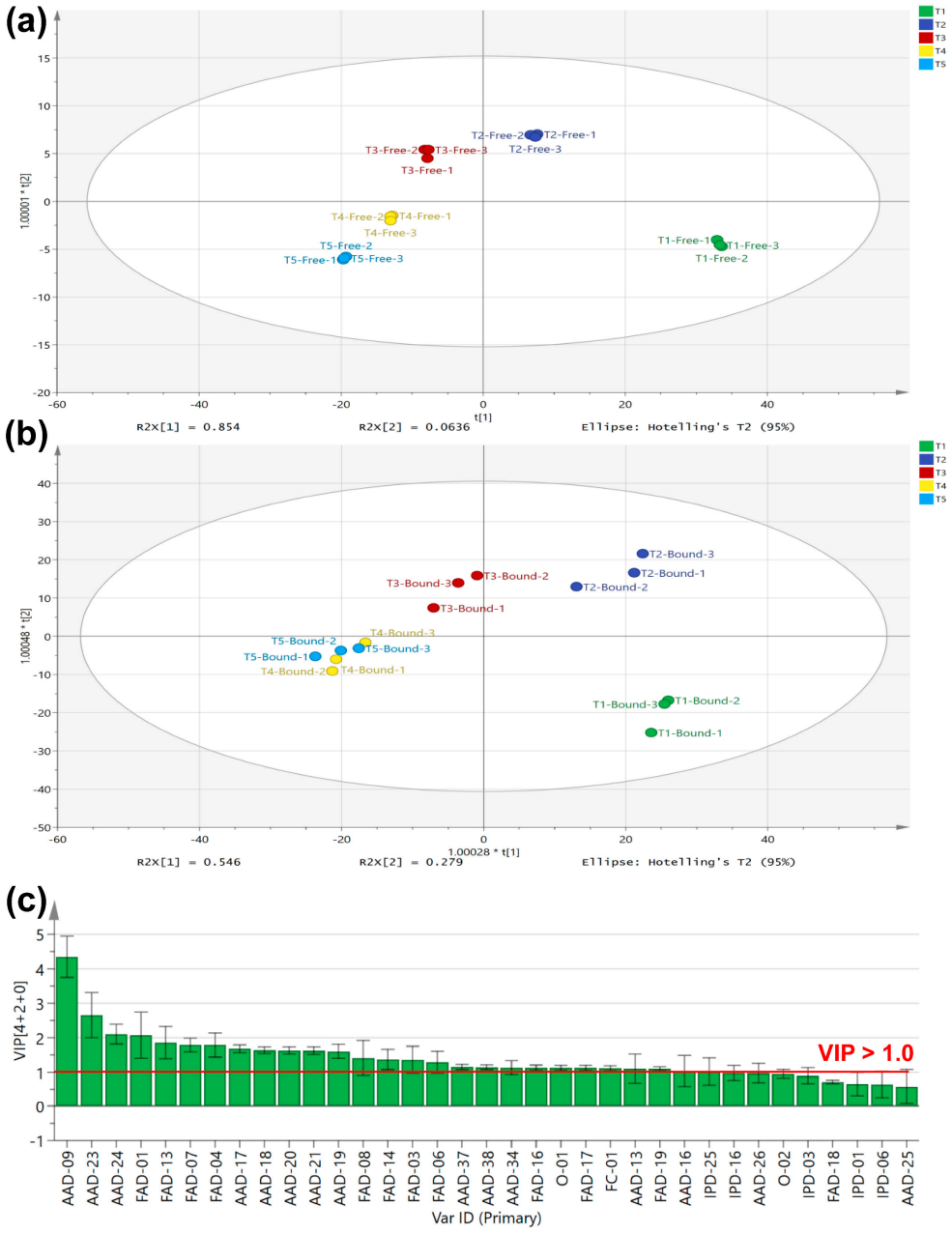

Figure 7. OPLS−DA score scatter plots of free (**a**) and bound (**b**) forms of volatiles expressed as ng/berry, and the key parameters with VIP scores above 1.0 (**c**) during on-vine grape dehydration. T1, T2, T3, T4, and T5 represent the sampling points at different dehydration degrees. The corresponding compounds for the abbreviations are listed in Tables S1 and S2.

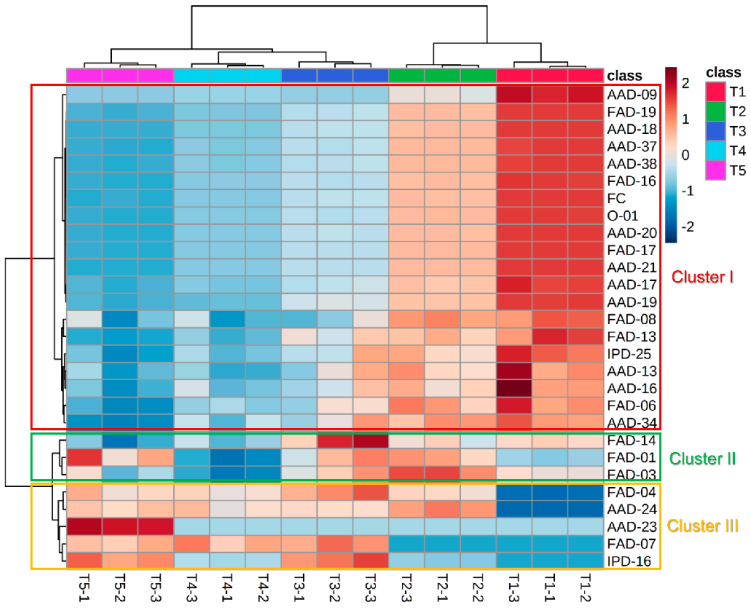

Figure 8. Hierarchical cluster heatmap of free volatiles expressed as ng/berry with VIP > 1.0 in OPLS−DA. T1, T2, T3, T4, and T5 represent the sampling points at different dehydration degrees. The corresponding compounds for the abbreviations are listed in Tables S1 and S2.

Among the free-form volatiles in the early stage of dehydration (T1), 2,4-di-*tert*-butylphenol was the main component of volatile phenols and AADs, with its content accounting for 99.07% and 32.43% of the total amount of these two groups in a single berry, respectively (Table S2). The content of this compound decreased rapidly during the dehydration process and, at the end of the dehydration (T5), its content had decreased to 27.33% and 0.20% in volatile phenols and AADs, respectively. Unlike most of the volatiles, the content of 2,4-di-*tert*-butylphenol in juice (μg/L) still decreased rapidly even under the concentration effect of dehydration (Table S1). This compound has also been detected by some authors in wine [49,50], distilled spirits [51], and other fruits [52] or fruit wines [53]. In addition to fruits, 2,4-di-*tert*-butylphenol is widely produced in microorganisms [54], medicinal plants [55], rice [46], and even some animals [56]. As a lipophilic volatile phenol, 2,4-di-*tert*-butylphenol possesses strong antioxidant [55,56] and antifungal activities [57], and it may be generated by the synthesis of phenylalanine through the shikimic acid pathway or by the degradation of eugenol or isoeugenol [55]. Gao et al. (2018) have reported the powerful inhibitory effect of 2,4-di-*tert*-butylphenol against fruit (i.e., peach and lychee) fungal pathogens [54]. In a subsequent study, the same team found that 2,4-di-*tert*-butylphenol could induce the production of antioxidant and disease-resistant enzymes in lychee fruit and destroy the structure of fungal cells, effectively inducing postharvest disease resistance in lychee fruits and resisting fungal attack [57]. Zhao et al. (2020) have speculated that the primary biological function of the highly toxic secondary metabolite 2,4-di-*tert*-butylphenol may be to act as an endocide (endogenous biocide) involved in the endocidal regulation of its producers [56,58]. Therefore, we inferred that the high content of 2,4-di-*tert*-butylphenol appearing at T1 might have been related to the induction of fungal pathogens caused by the rainfall and relatively high humidity at the beginning of dehydration (Figure S1, T1), and then gradually degraded under dry weather conditions without fungal infection.

Another important metabolic marker with notable rose and honey aroma was 2-phenethyl acetate. As mentioned before, both the free and bound forms of this compound were improved dramatically at the end of dehydration (T5; Figure 5). With the content (μg/L) exceeding its threshold, this volatile might be a key sensorial marker of the final wine made from highly dehydrated grapes. It has been well-demonstrated that 2-phenethyl acetate is a key contributor to the nut, rose, and honey notes of Vidal icewine, and was detected in both grapes and the corresponding wines [31,59,60]. Chen et al. (2019) have

found that 2-phenethyl acetate fluctuated during the late-harvest freeze–thaw cycle in Vidal grapes, and was present in higher levels in on-vine than off-vine samples at the end of harvest [31]. They hypothesized that biosynthesis and degradation occur simultaneously on this compound during late-harvest. A significant improvement in 2-phenethyl acetate was also observed at the end of the on-vine non-destructive dehydration in our study (Figure 5), indicating that the synthesis of this compound also took place in grapes at this period.

3.6. Further Discussion

Dessert wines made from on-vine late-harvest or off-vine postharvest dehydrated grapes are widely produced in the world, including some wine regions of China. The evolution patterns of volatile compounds during the late- or post-harvest periods and the effects of this process on aromatic compounds in grapes or wines have been extensively studied, especially in the past decade. Among the published reports, most of them have focused on the grape materials for botrytized wine and icewine, or grapes that undergo post-harvest dehydration, while few studies have focused specifically on non-destructive on-vine dehydration processes. Therefore, the data presented in this article provide a clear picture of the evolution of grape volatiles during this process.

For the quantitative analysis of grape aroma composition, as pointed out by D'Onofrio et al. [10], the expression of the content for volatiles should be chosen appropriately according to the purpose of the study. However, some studies appeared to be somewhat haphazard in their choice regarding the expression and calculation of volatile content. In our results (Figure 3), the evolutionary patterns of volatiles during dehydration were completely different when represented in two separate ways, which strongly supported this viewpoint. When conducting similar research in the future, the expression of the volatile compounds content should be clarified first. For the readers, the same attention should also be paid when reviewing the literature. From this point of view, it is difficult to conclude whether the increases in grape volatiles (expressed in μg/L or other similar units) during dehydration or late-harvest in some articles could be attributed to the dehydration concentration effect or biotransformation. From the results of our study, it appears that the changes in volatiles during dehydration were the result of a combined effect of these factors.

The most representative products of late-harvest wines are botrytized wine and icewine, both of which are made from over-ripe grapes that had dehydrated and underwent berry structure destruction, to some extent. *Botrytis cinerea* infection is a specific and complex process that the grapes need to encounter—intentionally or unintentionally—during the late-harvest winemaking process. When the berry is infected by *Botrytis*, its cuticle is degraded by the mycelium, thus increasing its permeability, consequently leading to dehydration and wrinkling [10,33]. After infection, *Botrytis* alters the accumulation of grape secondary metabolites by inducing biotic and abiotic stress, or the defensive responses of the berry [47,61]. The main metabolites associated with *Botrytis* infection in grapes are 1-octen-3-ol, 4-terpineol, benzaldehyde, phenylacetaldehyde, furaneol, 2-hepten-1-ol, 3,5-octadien-2-one, sulcatol, vanillin, γ-butyrolactone, and γ-nonalactone, among others [32–34,47,62,63]. In fact, *Botrytis* infection is relatively common in icewine winemaking, and would result in modifications in the volatile composition of the grape and wine [21]. Of course, the role of the freeze–thaw cycle is irreplaceable in icewine-making, as this process leads to a series of biochemical and chemical reactions, including biotransformation, anaerobic metabolism, and oxidation, which produce significant changes in the volatiles of the berries, especially the C6 alcohols, higher alcohols, and oxidative terpene derivatives [19]. Based on our results, it appears that, although the grapes did not experience structural damage due to *Botrytis* infection and/or freeze–thaw cycles, the concentration effect caused by water loss during this non-destructive dehydration was not the only factor responsible for the variation in the volatiles. The evolution patterns of volatile compounds expressed as ng/berry in our study revealed that, although water-loss concentration played a considerable role during non-destructive dehydration, biosynthesis and biodegradation

also occurred during this process, which eventually modified some volatiles significantly, especially some powerful odorants such as hexanal, *trans*-2-hexenal, 2-phenethyl acetate, β-myrcene, linalool, geraniol, *cis*-rose oxide, and β-damascenone.

The results of this paper also suggest that the metabolic pattern of volatiles during on-vine dehydration is likely to fundamentally differ from that during post-harvest off-vine dehydration. Costantini et al. (2006) [20] have proposed that, during post-harvest off-vine dehydration, the grape cells shift from aerobic to anaerobic metabolism, which was marked by an increase in alcohol dehydrogenase (ADH) activity and the significant accumulation of ethanol. This rapid increase in ethanol has also observed in icewine grapes at the final stage of freeze–thaw cycling by other authors [19]. However, no significant accumulation of ethanol (ng/berry) was observed in our study (Table S2), suggesting that anaerobic metabolism of grape berries did not occur during on-vine non-destructive dehydration. Unlike destructive or off-vine dehydration, the structure of the grape berry during on-vine dehydration was not destroyed and metabolite exchange between the grape berry and vine was not cut off, such that the metabolic pattern might completely differ.

Of course, the gene expression of key odorants during on-vine dehydration and the influence of dehydration degree on wine quality—especially regarding the balance between grape yield and wine quality—needs to be further investigated.

4. Conclusions

Both free and glycosidically bound forms of volatile compounds in Vidal grapes from the Shangri-La high-altitude region during the on-vine non-destructive dehydration process were investigated in this study. After two months of on-vine dehydration, the sugar content and acidity of the grape juice were dramatically enhanced, while the berry weight and juice yield sharply decreased. Predominantly in the bound forms, FADs, AADs, and IPDs were the three main types of volatiles in dehydrated Vidal grapes. Although water-loss concentration played a considerable role during non-destructive dehydration, biosynthesis and biodegradation also occurred during this process, eventually modifying some volatiles significantly, especially for some powerful odorants such as hexanal, *trans*-2-hexenal, 2-phenethyl acetate, β-myrcene, linalool, geraniol, *cis*-rose oxide, and β-damascenone. The evolution pattern of the volatile compounds in on-vine non-destructive dehydration differed from that in destructive dehydration or post-harvest dehydration processes, as anaerobic metabolism of the grape berries did not occur during on-vine non-destructive dehydration in our study. The U-LRA results indicated that 1-octen-3-ol was relatively stable during the non-destructive on-vine dehydration process and its content in grape juice was mainly determined by the concentration effect. Twenty-seven free-form compounds with VIP values greater than 1.0 were screened by OPLS-DA as metabolic markers to discriminate the grapes at different dehydration degrees, among which 2,4-di-*tert*-butylphenol, 2-phenethyl acetate, 2-methyl-1-propanol, and hexanol, with VIP values above 2.0, were the most important metabolic markers. Our study also highlights the fundamental importance of the expression of volatile content in the metabolomic study of grape berries.

Supplementary Materials: The following supporting information can be downloaded at: https://www.mdpi.com/article/10.3390/horticulturae8111029/s1, Figure S1: Meteorological data during the sampling period of the vineyard; Figure S2: Visual appearance of the grapes after harvest at T5; Figure S3: PCA score scatter-plots of free (a) and bound (b) forms of volatiles, expressed as ng per berry; Figure S4: Permutation plots of samples at different dehydration degrees (T1, T2, T3, T4, and T5); Table S1: Volatile compounds detected in Vidal grapes grown in Weixi at different on-vine dehydration degrees expressed by μg/L.; Table S2: Volatile compounds detected in Vidal grapes grown in Weixi at different on-vine dehydration degrees, expressed by ng/berry.

Author Contributions: Conceptualization, Q.-F.X. and L.F.; methodology, Q.-F.X. and L.F.; investigation, K.-X.L.; resources, M.-X.Z.; software, D.-M.Z.; writing—original draft preparation, Q.-F.X.; writing—review and editing, L.F. and J.C.; supervision, M.-X.Z.; funding acquisition, J.C. All authors have read and agreed to the published version of the manuscript.

Funding: This research was funded by the Special Basic Cooperative Research Programs of Yunnan Provincial Undergraduate Universities' Association (grant NO. 2018FH001-040).

Data Availability Statement: The data presented in this study are available on request from the corresponding author. The data are not publicly available due to privacy.

Acknowledgments: All the authors thank Yunnan Zangdi Tianxiang Winery for supporting the grape sampling.

Conflicts of Interest: The authors declare no conflict of interest.

References

1. Hjelmeland, A.K.; Ebeler, S.E. Glycosidically Bound Volatile Aroma Compounds in Grapes and Wine: A Review. *Am. J. Enol. Vitic.* **2015**, *66*, 1–11. [CrossRef]
2. Ferreira, V.; Lopez, R. The Actual and Potential Aroma of Winemaking Grapes. *Biomolecules* **2019**, *9*, 818. [CrossRef] [PubMed]
3. Gonzalez-Barreiro, C.; Rial-Otero, R.; Cancho-Grande, B.; Simal-Gandara, J. Wine Aroma Compounds in Grapes: A Critical Review. *Crit. Rev. Food Sci. Nutr.* **2015**, *55*, 202–218. [CrossRef] [PubMed]
4. Robinson, A.L.; Boss, P.K.; Solomon, P.S.; Trengove, R.D.; Heymann, H.; Ebeler, S.E. Origins of Grape and Wine Aroma. Part 1. Chemical Components and Viticultural Impacts. *Am. J. Enol. Vitic.* **2014**, *65*, 1–24. [CrossRef]
5. Wei, X.-F.; Ma, X.-L.; Cao, J.-H.; Sun, X.-Y.; Fang, Y.-L. Aroma Characteristics and Volatile Compounds of Distilled Crystal Grape Spirits of Different Alcohol Concentrations: Wine Sprits in the Shangri-La Region of China. *Food Sci. Technol.* **2018**, *38*, 50–58. [CrossRef]
6. Li, Z.; Pan, Q.-H.; Jin, Z.-M.; Mu, L.; Duan, C.-Q. Comparison on Phenolic Compounds in *Vitis Vinifera* Cv. Cabernet Sauvignon Wines from Five Wine-Growing Regions in China. *Food Chem.* **2011**, *125*, 77–83. [CrossRef]
7. Wang, X.Q.; Xie, X.L.; Chen, N.; Wang, H.; Li, H. Study on Current Status and Climatic Characteristics of Wine Regions in China. *Vitis* **2018**, *57*, 9–16. [CrossRef]
8. Zhao, P.; Gao, J.; Qian, M.; Li, H. Characterization of the Key Aroma Compounds in Chinese Syrah Wine by Gas Chromatography-Olfactometry-Mass Spectrometry and Aroma Reconstitution Studies. *Molecules* **2017**, *22*, 1045. [CrossRef]
9. Genovese, A.; Gambuti, A.; Piombino, P.; Moio, L. Sensory Properties and Aroma Compounds of Sweet Fiano Wine. *Food Chem.* **2007**, *103*, 1228–1236. [CrossRef]
10. Mencarelli, F.; Tonutti, P. *Sweet, Reinforced and Fortified Wines: Grape Biochemistry, Technology and Vinification*; John Wiley & Sons: Chichester, UK, 2013.
11. Noguerol-Pato, R.; Gonzalez-Alvarez, M.; Gonzalez-Barreiro, C.; Cancho-Grande, B.; Simal-Gandara, J. Evolution of the Aromatic Profile in Garnacha Tintorera Grapes During Raisining and Comparison with That of the Naturally Sweet Wine Obtained. *Food Chem.* **2013**, *139*, 1052–1061. [CrossRef]
12. Jackson, R.S. *Wine Science—Principles and Applications*, 3rd ed.; Elsevier: London, UK, 2008.
13. Giacosa, S.; Giordano, M.; Vilanova, M.; Cagnasso, E.; Segade, S.R.; Rolle, L. On-Vine Withering Process of 'Moscato Bianco' Grapes: Effect of Cane-Cut System on Volatile Composition. *J. Sci. Food Agric.* **2018**, *99*, 1135–1144. [CrossRef] [PubMed]
14. Bellincontro, A.; De Santis, D.; Botondi, R.; Villa, I.; Mencarelli, F. Different Postharvest Dehydration Rates Affect Quality Characteristics and Volatile Compounds of Malvasia, Trebbiano and Sangiovese Grapes for Wine Production. *J. Sci. Food Agric.* **2004**, *84*, 1791–1800. [CrossRef]
15. Javed, H.U.; Wang, D.; Wu, G.F.; Kaleem, Q.M.; Duan, C.Q.; Shi, Y. Post-Storage Changes of Volatile Compounds in Air- and Sun-Dried Raisins with Different Packaging Materials Using Hs-Spme with Gc/Ms. *Food Res. Int.* **2019**, *119*, 23–33. [CrossRef] [PubMed]
16. Cirilli, M.; Bellincontro, A.; De Santis, D.; Botondi, R.; Colao, M.C.; Muleo, R.; Mencarelli, F. Temperature and Water Loss Affect ADH Activity and Gene Expression in Grape Berry During Postharvest Dehydration. *Food Chem.* **2012**, *132*, 447–454. [CrossRef] [PubMed]
17. Chen, K.; Zhang, L.; Qiu, S.; Wu, X.G.; Li, J.M.; Ma, L.Y. Freeze-Thaw Cycles Characterize Varietal Aroma of Vidal Blanc Grape During Late Harvest by Shaping Self-Assembled Microeukaryotic Communities. *Food Chem.* **2022**, *384*, 132553. [CrossRef]
18. Franco, M.; Peinado, R.A.; Medina, M.; Moreno, J. Off-Vine Grape Drying Effect on Volatile Compounds and Aromatic Series in Must from Pedro Ximenez Grape Variety. *J. Agric. Food Chem.* **2004**, *52*, 3905–3910. [CrossRef]
19. Lan, Y.-B.; Qian, X.; Yang, Z.-J.; Xiang, X.-F.; Yang, W.-X.; Liu, T.; Zhu, B.-Q.; Pan, Q.-H.; Duan, C.-Q. Striking Changes in Volatile Profiles at Sub-Zero Temperatures During over-Ripening of 'Beibinghong' Grapes in Northeastern China. *Food Chem.* **2016**, *212*, 172–182. [CrossRef]
20. Costantini, V.; Bellincontro, A.; De Santis, D.; Botondi, R.; Mencarelli, F. Metabolic Changes of Malvasia Grapes for Wine Production During Postharvest Drying. *J. Agric. Food Chem.* **2006**, *54*, 3334–3340. [CrossRef]
21. Ma, Y.; Xu, Y.; Tang, K. Aroma of Icewine: A Review on How Environmental, Viticultural, and Oenological Factors Affect the Aroma of Icewine. *J. Agric. Food Chem.* **2021**, *69*, 6943–6957. [CrossRef]
22. *GB/T15038-2006*; Analytical Methods of Wine and Fruit Wine (State Administration for Market Regulation of China). China Standard Press: Beijing, China, 2006.

23. Ruiz, M.J.; Zea, L.; Moyano, L.; Medina, M. Aroma Active Compounds During the Drying of Grapes Cv. Pedro Ximenez Destined to the Production of Sweet Sherry Wine. *Eur. Food Res. Technol.* **2010**, *230*, 429–435. [CrossRef]
24. Reboredo-Rodríguez, P.; González-Barreiro, C.; Rial-Otero, R.; Cancho-Grande, B.; Simal-Gándara, J. Effects of Sugar Concentration Processes in Grapes and Wine Aging on Aroma Compounds of Sweet Wines-a Review. *Crit. Rev. Food Sci. Nutr.* **2015**, *55*, 1053–1073. [CrossRef] [PubMed]
25. Bowen, A.J.; Reynolds, A.G. Aroma Compounds in Ontario Vidal and Riesling Icewines. I. Effects of Harvest Date. *Food Res. Int.* **2015**, *76*, 540–549. [CrossRef]
26. Chkaiban, L.; Botondi, R.; Bellicontro, A.; De Santis, D.; Kefalas, P.; Mencarelli, F. Influence of Postharvest Water Stress on Lipoxygenase and Alcohol Dehydrogenase Activities, and on the Composition of Some Volatile Compounds of Gewurztraminer Grapes Dehydrated under Controlled and Uncontrolled Thermohygrometric Conditions. *Aust. J. Grape Wine Res.* **2007**, *13*, 142–149. [CrossRef]
27. Pan, Q.-H.; Chen, F.; Zhu, B.-Q.; Ma, L.-Y.; Li, L.; Li, J.-M. Molecular Cloning and Expression of Gene Encoding Aromatic Amino Acid Decarboxylase in 'Vidal Blanc' Grape Berries. *Mol. Biol. Rep.* **2012**, *39*, 4319–4325. [CrossRef] [PubMed]
28. van Gemert, L.J. *Odour Thresholds Compilations of Odour Threshold Values in Air, Water and Other Media*, 2nd ed.; Oliemans, Punter & Partners BV: Zeist, The Netherlands, 2011.
29. Zhu, J.-C.; Chen, F.; Wang, L.-Y.; Niu, Y.-W.; Xiao, Z.-B. Evaluation of the Synergism among Volatile Compounds in Oolong Tea Infusion by Odour Threshold with Sensory Analysis and E-Nose. *Food Chem.* **2017**, *221*, 1484–1490. [CrossRef]
30. Chou, H.C.; Suklje, K.; Antalick, G.; Schmidtke, L.M.; Blackman, J.W. Late-Season Shiraz Berry Dehydration That Alters Composition and Sensory Traits of Wine. *J. Agric. Food Chem.* **2018**, *66*, 7750–7757. [CrossRef]
31. Chen, K.; Wen, J.F.; Ma, L.Y.; Wen, H.C.; Li, J.M. Dynamic Changes in Norisoprenoids and Phenylalanine-Derived Volatiles in Off-Vine Vidal Blanc Grape During Late Harvest. *Food Chem.* **2019**, *289*, 645–656. [CrossRef]
32. Simonato, B.; Lorenzini, M.; Cipriani, M.; Finato, F.; Zapparoli, G. Correlating Noble Rot Infection of Garganega Withered Grapes with Key Molecules and Odorants of Botrytized Passito Wine. *Foods* **2019**, *8*, 642. [CrossRef]
33. Negri, S.; Lovato, A.; Boscaini, F.; Salvetti, E.; Torriani, S.; Commisso, M.; Danzi, R.; Ugliano, M.; Polverari, A.; Tornielli, G.B.; et al. The Induction of Noble Rot (*Botrytis cinerea*) Infection During Postharvest Withering Changes the Metabolome of Grapevine Berries (*Vitis vinifera* L., Cv. Garganega). *Front. Plant Sci.* **2017**, *8*, 12. [CrossRef]
34. Tosi, E.; Fedrizzi, B.; Azzolini, M.; Finato, F.; Simonato, B.; Zapparoli, G. Effects of Noble Rot on Must Composition and Aroma Profile of Amarone Wine Produced by the Traditional Grape Withering Protocol. *Food Chem.* **2012**, *130*, 370–375. [CrossRef]
35. D'Onofrio, C.; Matarese, F.; Scalabrelli, G.; Boss, P.K. Functional Characterization of Terpene Synthases of 'Aromatic' and 'Non-Aromatic' Grapevine Cultivars. In Proceedings of the X International Conference on Grapevine Breeding and Genetics, Geneva, NY, USA, 1–5 August 2010; pp. 557–563.
36. Segade, S.R.; Vilanova, M.; Giacosa, S.; Perrone, I.; Chitarra, W.; Pollon, M.; Torchio, F.; Boccacci, P.; Gambino, G.; Gerbi, V.; et al. Ozone Improves the Aromatic Fingerprint of White Grapes. *Sci. Rep.* **2017**, *7*, 16. [CrossRef] [PubMed]
37. Torchio, F.; Giacosa, S.; Vilanova, M.; Segade, S.R.; Gerbi, V.; Giordano, M.; Rolle, L. Use of Response Surface Methodology for the Assessment of Changes in the Volatile Composition of Moscato Bianco (*Vitis vinifera* L.) Grape Berries During Ripening. *Food Chem.* **2016**, *212*, 576–584. [CrossRef] [PubMed]
38. D'Onofrio, C.; Matarese, F.; Cuzzola, A. Study of the Terpene Profile at Harvest and During Berry Development of Vitis Vinifera L. Aromatic Varieties Aleatico, Brachetto, Malvasia Di Candia Aromatica and Moscato Bianco. *J. Sci. Food Agric.* **2017**, *97*, 2898–2907. [CrossRef]
39. Crespo, J.; Rigou, P.; Romero, V.; García, M.; Arroyo, T.; Cabellos, J.M. Effect of Seasonal Climate Fluctuations on the Evolution of Glycoconjugates During the Ripening Period of Grapevine Cv. Muscat à Petits Grains Blancs Berries. *J. Sci. Food Agric.* **2018**, *98*, 1803–1812. [CrossRef]
40. Mendes-Pinto, M.M. Carotenoid Breakdown Products the-Norisoprenoids-in Wine Aroma. *Arch. Biochem. Biophys.* **2009**, *483*, 236–245. [CrossRef] [PubMed]
41. Feng, H.; Yuan, F.; Skinkis, P.A.; Qian, M.C. Influence of Cluster Zone Leaf Removal on Pinot Noir Grape Chemical and Volatile Composition. *Food Chem.* **2015**, *173*, 414–423. [CrossRef] [PubMed]
42. Darriet, P.; Pons, M.; Henry, R.; Dumont, O.; Findeling, V.; Cartolaro, P.; Calonnec, A.; Dubourdieu, D. Impact Odorants Contributing to the Fungus Type Aroma from Grape Berries Contaminated by Powdery Mildew (*Uncinula necator*); Incidence of Enzymatic Activities of the Yeast Saccharomyces Cerevisiae. *J. Agric. Food Chem.* **2002**, *50*, 3277–3282. [CrossRef]
43. Bylesjö, M.; Rantalainen, M.; Cloarec, O.; Nicholson, J.K.; Holmes, E.; Trygg, J. OPLS Discriminant Analysis: Combining the Strengths of PLS-DA and Simca Classification. *J. Chemom.* **2006**, *20*, 341–351. [CrossRef]
44. Triba, M.N.; Le Moyec, L.; Amathieu, R.; Goossens, C.; Bouchemal, N.; Nahon, P.; Rutledge, D.N.; Savarin, P. PLS/OPLS Models in Metabolomics: The Impact of Permutation of Dataset Rows on the K-Fold Cross-Validation Quality Parameters. *Mol. Biosyst.* **2015**, *11*, 13–19. [CrossRef]
45. Wang, X.-Y.; Wang, H.-L.; Zhang, G.-J.; Yan, A.-L.; Ren, J.-C.; Liu, Z.-H.; Xu, H.-Y.; Sun, L. Effects of Fruit Bagging Treatment with Different Types of Bags on the Contents of Phenolics and Monoterpenes in Muscat-Flavored Table Grapes. *Horticulturae* **2022**, *8*, 411. [CrossRef]
46. Zhao, Q.; Xi, J.; Xu, D.; Jin, Y.; Wu, F.; Tong, Q.; Xu, X. Effect of Optimal-Water Boiling Cooking on the Volatile Compounds in 26 Japonica Rice Varieties from China. *Food Res. Int.* **2022**, *155*, 111078. [CrossRef] [PubMed]

47. Santos, H.; Augusto, C.; Reis, P.; Rego, C.; Figueiredo, A.C.; Fortes, A.M. Volatile Metabolism of Wine Grape Trincadeira: Impact of Infection with Botrytis Cinerea. *Plants* **2022**, *11*, 141. [CrossRef] [PubMed]
48. Wang, X.; Wu, Y.; Zhu, H.; Zhang, H.; Xu, J.; Fu, Q.; Bao, M.; Zhang, J. Headspace Volatiles and Endogenous Extracts of Prunus Mume Cultivars with Different Aroma Types. *Molecules* **2021**, *26*, 7256. [CrossRef] [PubMed]
49. Nan, L.; Liu, L.; Li, Y.; Huang, J.; Wang, Y.; Wang, C.; Wang, Z.; Xu, C. Comparison of Aroma Compounds in Cabernet Sauvignon Red Wines from Five Growing Regions in Xinjiang in China. *J. Food Qual.* **2021**, *2021*, 5562518. [CrossRef]
50. de Macêdo Morais, S.; de Sousa GalvÃO, M.; de Carvalho, L.M.; Olegario, L.S.; Pereira, G.E.; de Andrade Lima, L.L.; da Silva, F.L.H.; Madruga, M.S. Potential Typicality Marker of Volatile Composition of Commercial Sparkling Wines from the Caatinga Biome. *Food Anal. Method.* **2022**. [CrossRef]
51. Zhao, L.; Ruan, S.; Yang, X.; Chen, Q.; Shi, K.; Lu, K.; He, L.; Liu, S.; Song, Y. Characterization of Volatile Aroma Compounds in Litchi (Heiye) Wine and Distilled Spirit. *Food Sci. Nutr.* **2021**, *9*, 5914–5927. [CrossRef]
52. Amorim, C.; Alves Filho, E.G.; Rodrigues, T.H.S.; Bender, R.J.; Canuto, K.M.; Garruti, D.S.; Antoniolli, L.R. Volatile Compounds Associated to the Loss of Astringency in 'Rama Forte' Persimmon Fruit. *Food Res. Int.* **2020**, *136*, 109570. [CrossRef]
53. Liu, J.; Liu, M.; Ye, P.; Lin, F.; Huang, J.; Wang, H.; Zhou, R.; Zhang, S.; Zhou, J.; Cai, L. Characterization of Major Properties and Aroma Profile of Kiwi Wine Co-Cultured by Saccharomyces Yeast (*S. Cerevisiae*, *S. Bayanus*, *S. Uvarum*) and T. Delbrueckii. *Eur. Food Res. Technol.* **2020**, *246*, 807–820. [CrossRef]
54. Gao, H.; Li, P.; Xu, X.; Zeng, Q.; Guan, W. Research on Volatile Organic Compounds from Bacillus Subtilis Cf-3: Biocontrol Effects on Fruit Fungal Pathogens and Dynamic Changes During Fermentation. *Front. Microbiol.* **2018**, *9*, 456. [CrossRef]
55. Ali, A.; Chong, C.H.; Mah, S.H.; Abdullah, L.C.; Choong, T.S.Y.; Chua, B.L. Impact of Storage Conditions on the Stability of Predominant Phenolic Constituents and Antioxidant Activity of Dried Piper Betle Extracts. *Molecules* **2018**, *23*, 484. [CrossRef]
56. Zhao, F.; Wang, P.; Lucardi, R.D.; Su, Z.; Li, S. Natural Sources and Bioactivities of 2,4-Di-Tert-Butylphenol and Its Analogs. *Toxins* **2020**, *12*, 35. [CrossRef] [PubMed]
57. Zhao, P.; Li, P.; Wu, S.; Zhou, M.; Zhi, R.; Gao, H. Volatile Organic Compounds (VOCs) from Bacillus Subtilis Cf-3 Reduce Anthracnose and Elicit Active Defense Responses in Harvested Litchi Fruits. *AMB Express* **2019**, *9*, 119. [CrossRef] [PubMed]
58. Li, S.; Wang, P.; Yuan, W.; Su, Z.; Bullard, S.H. Endocidal Regulation of Secondary Metabolites in the Producing Organisms. *Sci. Rep.* **2016**, *6*, 29315. [CrossRef]
59. Ge, Q.; Guo, C.; Yan, Y.; Sun, X.; Ma, T.; Zhang, J.; Li, C.; Gou, C.; Yue, T.; Yuan, Y. Contribution of Non-Saccharomyces Yeasts to Aroma-Active Compound Production, Phenolic Composition and Sensory Profile in Chinese Vidal Icewine. *Food Biosci.* **2022**, *46*, 101152. [CrossRef]
60. Huang, L.; Ma, Y.; Tian, X.; Li, J.M.; Li, L.X.; Tang, K.; Xu, Y. Chemosensory Characteristics of Regional Vidal Icewines from China and Canada. *Food Chem.* **2018**, *261*, 66–74. [CrossRef] [PubMed]
61. Blanco-Ulate, B.; Amrine, K.C.H.; Collins, T.S.; Rivero, R.M.; Vicente, A.R.; Morales-Cruz, A.; Doyle, C.L.; Ye, Z.; Allen, G.; Heymann, H.; et al. Developmental and Metabolic Plasticity of White-Skinned Grape Berries in Response to Botrytis Cinerea During Noble Rot. *Plant Physiol.* **2015**, *169*, 2422–2443. [CrossRef]
62. Furdikova, K.; Machynakova, A.; Drtilova, T.; Klempova, T.; Durcanska, K.; Spanik, I. Comparison of Volatiles in Noble-Rotten and Healthy Grape Berries of Tokaj. *Lwt-Food Sci. Technol.* **2019**, *105*, 37–47. [CrossRef]
63. Lopez Pinar, A.; Rauhut, D.; Ruehl, E.; Buettner, A. Effects of Botrytis Cinerea and Erysiphe Necator Fungi on the Aroma Character of Grape Must: A Comparative Approach. *Food Chem.* **2016**, *207*, 251–260. [CrossRef]